using mice received approval from the Kazusa DNA Research Institute Administrative Panel for Animal Care. All animal care was conducted in accordance with the guidelines of the Kazusa DNA Research Institute.

CD4 T cells differentiation *in vitro*

Naïve CD4 T ($CD44^{lo}CD62L^{hi}$) cells were prepared using a $CD4^{+}CD62L^{+}$ T cell isolation kit II (Miltenyi Biotec). Naïve CD4 T cells (1.5×10^{6}) were stimulated with an immobilized anti-TCR-β mAb (3 μg/ml; H57-597; BioLegend) and an anti-CD28 mAb (1 μg/ml; 37.5; BioLegend) with or without SH-2251 (Ishihara Sangyo Kaisha, Ltd.) under the indicated culture conditions for two days. Next, the cells were transferred onto a new plate and cultured for an additional three days in the presence of cytokines with or without SH-2251. If not mentioned, 100 nM of SH-2251 was used in the experiments. The cytokine conditions for Th2 cell differentiation were as follows: IL-2 (2.5 ng/ml), IL-4 (10 ng/ml; PeproTech) and anti-IFN-γ mAb (5 μg/ml; R4-6A2; BioLegend).

Intracellular staining of cytokines

The *in vitro* differentiated Th cells were stimulated with an immobilized anti-TCR-β mAb (3 μg/ml; H57-597; BioLegend) for six hours in the presence of monensin (1 μM), and intracellular staining was performed as previously described [25]. The following antibodies were used for intracellular staining: anti-IL-4-hycoerythrin (PE) mAb (11B11; BD Bioscience), IFN-γ-FITC mAb (XMG1.2; BD Bioscience), IL-5-allophycocyanin (APC) (TRFK5; eBioscience), and IL-13-PE (eBio13A; eBioscience). A flow cytometric analysis was performed using a FACSCalibur instrument (BD biosciences), and the results were analyzed using the FlowJo software program (Tree Star).

ELISA

The cells were stimulated with an immobilized anti-TCR-β mAb for 16 hours, and the culture supernatants were recovered. The amount of cytokines in the recovered supernatants was determined with ELISA, as described previously [43].

Quantitative RT-PCR

Total RNA was isolated using a TRIZOL Reagent (GIBCO). cDNA was synthesized using the Superscript VILO cDNA synthesis kit (Invitrogen). Quantitative RT-PCR was performed as previously described [43], using StepOnePlus Real-Time PCR Systems (Applied Biosystems). The specific primers, and Roche Universal Probes used in the experiments were as follows:

Hprt: 5′ TCCTCCTCAGACCGCTTT 3′ (forward), 5′ CCTGTTCATCATCGTAATC 3′ (reverse), probe #95; *Gata3*: 5′ TTATCAAGCCCAAGCGAAG 3′ (forward), TGGTGGTGGTCTGACAGTT 3′ (reverse), probe #108; *Gfi1*: 5′ TCCGAGTTCGAGGACTTTG 3′ (forward), 5′ GAGCGGCACAGTGACTTCT 3′ (reverse), probe #7.

Microarray analysis

The gene expression profiles of the SH-2251-treated Th2 cells were analyzed using the Agilent Whole Mouse 44K Array. The raw data were subjected to log2 transformation and normalized using the Subio Platform (Subio). The gene expression data were deposited in the GSE42131.

Chromatin Immunoprecipitation (ChIP) assay and ChIP-sequencing

The Magna ChIP kit was used for the ChIP assay according to the manufacturer's protocol (MILLIPORE). The anti-histone H3K4me2 pAb (ab7766; Abcam), anti-histone H3K4me3 pAb (cat#39159; Activemotif), anti-histone H3K27me3 pAb (cat#39155; Activemotif), anti-histone H3K36me3 pAb (ab9050; Abcam), anti-histone H3K9ac pAb (cat#39137; ActiveMotif), anti-histone H3K27ac pAb (cat#39133; ActiveMotif), anti-Gata3 (cat# AF2605; R&D) pAb and anti-Gfi1 (M-19; Santa Cruz) were used for immunoprecipitation. The specific primers at the Th2 cytokine gene locus and the Roche Universal probes used in the experiments were as follows: #1: 5′ ACGCTTCCGGAACTAGGG 3′ (forward), 5′ CGCTCTGGCATCTCGTTC 3′ (reverse), probe #38; #2 (G2): 5′ CAGATGTGATATGCGTACATGTAATTC 3′ (forward), 5′ TGAACTCCTGACCCTGCTTT 3′ (reverse), probe #79; #3: 5′ AGTGTCTGTCCCCCAGATCA 3′ (forward), 5′ GCTGCCTGGAACTTGGTG 3′ (reverse), probe #64; #4: (Il5p), 5′ TCACTTTATCAGGAATTGAGTTTAACA 3′ (forward), 5′ GATCGGCTTTTCTTGAGCA 3′ (reverse), probe #43; #5: 5′ TGCCTCTCTTTGTTTTCCTTG 3′ (forward), 5′ GCAATTCAGTGGTAGAGT

GCTCA 3′ (reverse), probe #81; #6 (G4): 5′ AGTACAAGGGCCAAGTCACG 3′ (forward), 5′ GCCAGAGACTGGGGGTAAGT 3′ (reverse), probe #16; #7: 5′ GCTGGCCTTGAACTTACTACG 3′ (forward), 5′ GTGTGTACCCGTAATCCCA

AC 3′ (reverse), probe #10; G1: 5′ GGAAGTGGGAGTCCTAAGCA 3′ (forward), 5′ CTCCCTGCCCAACTTCTAAA 3′ (reverse), probe #15; G3: 5′ AAGGGGAGAACTGCCTCCTA 3′ (forward), 5′ TCATGCCATGGGATACAGG (reverse), prove #99; Il4p: 5′ TTGGTCTGATTTCACAGGAAAA 3′ (forward), 5′ GGCCAATCAGCACCTCTCT 3′ (reverse), probe #2; V_A site in the IL-4 enhancer: 5′ GCCTGTTTCCTCTCAGCATT 3′ (forward), 5′ TGATAAAAGTGACTTGAAGGTT

GG 3′ (reverse), probe #4; IL-4 intronic enhancer: 5′ CCCAAAGGAGGTGCTTTT

ATC 3′ (forward), 5′ AAATCCGAAACTGAGGAGTGC 3′ (reverse), probe #75; Il13p: 5′ CCAGGTTCTGGGTGGTTTATT 3′ (forward), 5′ GAATTACTGGGGCGGAAGTT 3′ (reverse), probe #105; Rad50p: 5′ GGAAGTGGGAGTCCTAAGCA 3′ (forward), 5′ CTCCCTGCCCAACTTCTAAA 3′ (reverse), probe #15. The specific primers at the Gfi1 gene locus and the Roche Universal probes used in the experiments were as follows:

a: 5′ TTTGCAGAAGAGTGAGGTTTGA 3′ (forward), 5′ TGGAGGCGTGGGATTAAC 3′ (reverse), probe #55; b: 5′ GACCAAGGCGTGTGA

CTATACA 3′ (forward), 5′ CACACCCTGTTGTACCCACTT 3′ (reverse), probe #48; c: 5′ GTGCCACACCACTATTCCAG 3′ (forward), 5′ AGTGGCAAAGGACCAAC

ACT 3′ (reverse), probe #2; d: 5′ TGGGGACAGGTTTTACCACT 3′ (forward), 5′ GACAGGTGGCACGAATCC 3′ (reverse), probe #70.

The samples for the ChIP-sequencing were prepared according to the manufacturer's protocol (Illumina), and the ChIP-sequence was performed using Genome Analyzer IIx (Illumina).

Immunoblot analysis

Cytoplasmic and nuclear extracts were prepared using NE-PER Nuclear and Cytoplasmic Extraction Regents (Thermo Fisher Scientific) as previously described [43]. Anti-Gata3 mAb (HG3-31; Santa Cruz), anti-Gfi1 pAb (M-19; Santa Cruz) and anti-α-Tubulin mAb (DM1A; Lab Vision) were used for the immunoblot analysis.

Retrovirus-mediated gene transfer

The methods for generating retrovirus supernatant and infection were described previously [25]. Infected cells were detected using staining with anti-human NGFR-PE mAb (ME20.4-1.H4; Miltenyi Biotec) and anti-PE microbeads (#130-048-801; Miltenyi Biotec), and hNGFR-positive infected cells were purified using AutoMACS (Miltenyi Biotec).

Luciferase assay

The IL-5 promoter activity was determined as previously described [30]. In brief, M12 cells (B cell line) were cotransfected with a firefly luciferase reporter (pGL3-*Il5* promoter), a renila luciferase plasmid (pRL-TK; Promega) and an expression vector (pFlag-CMV2; Sigma) using Gene Pulser MXcell (BIO-RAD). Twenty-four hours after transfection, the cells were maintained in the presence or absence of SH-2251 for one hour, and then stimulated with PMA plus dibuteryl-cAMP for 12 hours. The luciferase activity was measured using a Dual-Luciferase Reporter Assay System (Promega).

OVA-induced allergic airway inflammation

BALB/c mice were immunized intraperitoneally with 100 μg OVA in 2 mg of aluminum hydroxide gel on day 0. Next, the mice were intranasally challenged with OVA in saline (100 μg/mouse) on days 8 and 10. SH-2251 (10 mg/kg) was orally administered every day from day 0 to day 11. Two days after the last OVA challenge, BAL fluid cells and lung samples were prepared for histological examination as previously described [44]. Lung mononuclear cells were also prepared two days after the last OVA challenge, as previously described [45]. CD4 T cells were purified from lung mononuclear cells using anti-mouse CD4 microbeads (Miltenyi Biotec).

Statistical analysis

Student's *t*-test was used for the statistical analyses. ANOVA and the Bonferroni-test were used in the *in vivo* experiments.

Supporting Information

File S1 The effects of SH-2251 on Th1-, Th9-, and Th17-differentiation. Naïve CD4 T cells were cultured under Th1- (A), Th9- (B) or Th17- (C) conditions in the presence or absence of SH-2251 (100 nM) for five days. The cells were restimulated with an immobilized anti-TCR-β mAb for six hours, and the intracellular staining profiles were determined using intracellular staining (left). The following antibodies were used for intracellular staining: anti-IL-4-PE mAb (11B11; BD Bioscience), IFN-γ-FITC mAb (XMG1.2; BD Bioscience), anti-IL-9-PE mAb (RM9A4; BioLegend), anti-IL-17A-Alexa647 mAb (TC11-18H10.1; BioLegend) and IL-17F-Alexa488 mAb (9D3.1C8; BioLegend). The percentages of each quadrant are indicated. The cytokine production by the SH-2251-treated Th cells stimulated with an immobilized anti-TCR-β mAb for 16 hours was determined with ELISA. The culture conditions for each Th cell differentiations were as follows. Th1-conditions: IL-2 (2.5 ng/ml), IL-12 (1 ng/ml; PeproTech) and anti-IL-4 mAb (5 μg/ml; 11B11; BioLegend). Th9-conditions: IL-2 (2.5 ng/ml), IL-4 (10 ng/ml), TGF-β (10 ng/ml; PeproTech) and anti-IFN-γ mAb (5 μg/ml). The Th17-conditions were as follows: IL-6 (10 ng/ml; PeproTech), IL-1β (5 ng/ml; PeproTech), TGF-β (1 ng/ml), anti-IL-2 (5 μg/ml; BioLegend), anti-IL-4 mAb (5 μg/ml) and anti-IFN-γ mAb. Three independent experiments were performed with similar results. $*P<0.05$ and $**P<0.01$ (Student's *t*-test).
(DOCX)

Acknowledgments

We thank, Mr. Takashi Watanabe, Mr. Kazuhiro Sato, Mr. Masaki Takazawa, Ms. Yasuyo Tanaka and Ms. Noriko Nakashio for their excellent technical assistance.

Author Contributions

Conceived and designed the experiments: JS MY. Performed the experiments: JS MK ST TN OO MY. Analyzed the data: JS MK. Contributed reagents/materials/analysis tools: MI FK. Wrote the paper: JS MY.

References

1. Adcock IM, Caramori G, Chung KF (2008) New targets for drug development in asthma. Lancet 372: 1073–1087.
2. Holgate ST (2008) Pathogenesis of asthma. Clin Exp Allergy 38: 872–897.
3. Bosnjak B, Stelzmueller B, Erb KJ, Epstein MM (2011) Treatment of allergic asthma: modulation of Th2 cells and their responses. Respir Res 12: 114.
4. Kouro T, Takatsu K (2009) IL-5- and eosinophil-mediated inflammation: from discovery to therapy. Int Immunol 21: 1303–1309.
5. Rothenberg ME, Hogan SP (2006) The eosinophil. Annu Rev Immunol 24: 147–174.
6. Gauvreau GM, Ellis AK, Denburg JA (2009) Haemopoietic processes in allergic disease: eosinophil/basophil development. Clin Exp Allergy 39: 1297–1306.
7. Foster PS, Hogan SP, Ramsay AJ, Matthaei KI, Young IG (1996) Interleukin 5 deficiency abolishes eosinophilia, airways hyperreactivity, and lung damage in a mouse asthma model. J Exp Med 183: 195–201.
8. Wei L, Vahedi G, Sun HW, Watford WT, Takatori H, et al. (2010) Discrete roles of STAT4 and STAT6 transcription factors in tuning epigenetic modifications and transcription during T helper cell differentiation. Immunity 32: 840–851.
9. Ansel KM, Djuretic I, Tanasa B, Rao A (2006) Regulation of Th2 differentiation and Il4 locus accessibility. Annu Rev Immunol 24: 607–656.
10. Wilson CB, Rowell E, Sekimata M (2009) Epigenetic control of T-helper-cell differentiation. Nat Rev Immunol 9: 91–105.
11. Nakayama T, Yamashita M (2008) Initiation and maintenance of Th2 cell identity. Curr Opin Immunol 20: 265–271.
12. Zhu J, Yamane H, Paul WE (2010) Differentiation of effector CD4 T cell populations (*). Annu Rev Immunol 28: 445–489.
13. Taniguchi M, Tashiro T, Dashtsoodol N, Hongo N, Watarai H (2010) The specialized iNKT cell system recognizes glycolipid antigens and bridges the innate and acquired immune systems with potential applications for cancer therapy. Int Immunol 22: 1–6.
14. Neill DR, Wong SH, Bellosi A, Flynn RJ, Daly M, et al. (2010) Nuocytes represent a new innate effector leukocyte that mediates type-2 immunity. Nature 464: 1367–1370.
15. Moro K, Yamada T, Tanabe M, Takeuchi T, Ikawa T, et al. (2010) Innate production of T(H)2 cytokines by adipose tissue-associated c-Kit(+)Sca-1(+) lymphoid cells. Nature 463: 540–544.
16. Ikutani M, Yanagibashi T, Ogasawara M, Tsuneyama K, Yamamoto S, et al. (2012) Identification of innate IL-5-producing cells and their role in lung eosinophil regulation and antitumor immunity. J Immunol 188: 703–713.
17. Bartemes KR, Iijima K, Kobayashi T, Kephart GM, McKenzie AN, et al. (2012) IL-33-responsive lineage- CD25+ CD44(hi) lymphoid cells mediate innate type 2 immunity and allergic inflammation in the lungs. J Immunol 188: 1503–1513.
18. Halim TY, Krauss RH, Sun AC, Takei F (2012) Lung natural helper cells are a critical source of Th2 cell-type cytokines in protease allergen-induced airway inflammation. Immunity 36: 451–463.
19. Poon AH, Eidelman DH, Martin JG, Laprise C, Hamid Q (2012) Pathogenesis of severe asthma. Clin Exp Allergy 42: 625–637.
20. Moroy T, Khandanpour C (2011) Growth factor independence 1 (Gfi1) as a regulator of lymphocyte development and activation. Semin Immunol 23: 368–378.
21. Montoya-Durango DE, Velu CS, Kazanjian A, Rojas ME, Jay CM, et al. (2008) Ajuba functions as a histone deacetylase-dependent co-repressor for autoregulation of the growth factor-independent-1 transcription factor. J Biol Chem 283: 32056–32065.
22. Saleque S, Kim J, Rooke HM, Orkin SH (2007) Epigenetic regulation of hematopoietic differentiation by Gfi-1 and Gfi-1b is mediated by the cofactors CoREST and LSD1. Mol Cell 27: 562–572.
23. Duan Z, Zarebski A, Montoya-Durango D, Grimes HL, Horwitz M (2005) Gfi1 coordinates epigenetic repression of p21Cip/WAF1 by recruitment of histone

lysine methyltransferase G9a and histone deacetylase 1. Mol Cell Biol 25: 10338–10351.
24. Zhu J, Guo L, Min B, Watson CJ, Hu-Li J, et al. (2002) Growth factor independent-1 induced by IL-4 regulates Th2 cell proliferation. Immunity 16: 733–744.
25. Shinnakasu R, Yamashita M, Kuwahara M, Hosokawa H, Hasegawa A, et al. (2008) Gfi1-mediated stabilization of GATA3 protein is required for Th2 cell differentiation. J Biol Chem 283: 28216–28225.
26. Northrup DL, Zhao K (2011) Application of ChIP-Seq and related techniques to the study of immune function. Immunity 34: 830–842.
27. Bannister AJ, Kouzarides T (2011) Regulation of chromatin by histone modifications. Cell Res 21: 381–395.
28. Agarwal S, Avni O, Rao A (2000) Cell-type-restricted binding of the transcription factor NFAT to a distal IL-4 enhancer in vivo. Immunity 12: 643–652.
29. Tanaka S, Motomura Y, Suzuki Y, Yagi R, Inoue H, et al. (2011) The enhancer HS2 critically regulates GATA-3-mediated Il4 transcription in T(H)2 cells. Nat Immunol 12: 77–85.
30. Yamashita M, Ukai-Tadenuma M, Kimura M, Omori M, Inami M, et al. (2002) Identification of a conserved GATA3 response element upstream proximal from the interleukin-13 gene locus. J Biol Chem 277: 42399–42408.
31. Lee GR, Spilianakis CG, Flavell RA (2005) Hypersensitive site 7 of the TH2 locus control region is essential for expressing TH2 cytokine genes and for long-range intrachromosomal interactions. Nat Immunol 6: 42–48.
32. Lee GR, Fields PE, Griffin TJ, Flavell RA (2003) Regulation of the Th2 cytokine locus by a locus control region. Immunity 19: 145–153.
33. Schwenger GT, Fournier R, Kok CC, Mordvinov VA, Yeoman D, et al. (2001) GATA-3 has dual regulatory functions in human interleukin-5 transcription. J Biol Chem 276: 48502–48509.
34. Abonia JP, Putnam PE (2011) Mepolizumab in eosinophilic disorders. Expert Rev Clin Immunol 7: 411–417.
35. Haldar P, Brightling CE, Hargadon B, Gupta S, Monteiro W, et al. (2009) Mepolizumab and exacerbations of refractory eosinophilic asthma. N Engl J Med 360: 973–984.
36. Hurst SD, Muchamuel T, Gorman DM, Gilbert JM, Clifford T, et al. (2002) New IL-17 family members promote Th1 or Th2 responses in the lung: in vivo function of the novel cytokine IL-25. J Immunol 169: 443–453.
37. Ballantyne SJ, Barlow JL, Jolin HE, Nath P, Williams AS, et al. (2007) Blocking IL-25 prevents airway hyperresponsiveness in allergic asthma. J Allergy Clin Immunol 120: 1324–1331.
38. Terashima A, Watarai H, Inoue S, Sekine E, Nakagawa R, et al. (2008) A novel subset of mouse NKT cells bearing the IL-17 receptor B responds to IL-25 and contributes to airway hyperreactivity. J Exp Med 205: 2727–2733.
39. Yamashita M, Shinnakasu R, Asou H, Kimura M, Hasegawa A, et al. (2005) Ras-ERK MAPK cascade regulates GATA3 stability and Th2 differentiation through ubiquitin-proteasome pathway. J Biol Chem 280: 29409–29419.
40. Ito K, Caramori G, Lim S, Oates T, Chung KF, et al. (2002) Expression and activity of histone deacetylases in human asthmatic airways. Am J Respir Crit Care Med 166: 392–396.
41. Cosio BG, Mann B, Ito K, Jazrawi E, Barnes PJ, et al. (2004) Histone acetylase and deacetylase activity in alveolar macrophages and blood mononocytes in asthma. Am J Respir Crit Care Med 170: 141–147.
42. Khan AU, Krishnamurthy S (2005) Histone modifications as key regulators of transcription. Front Biosci 10: 866–872.
43. Kuwahara M, Yamashita M, Shinoda K, Tofukuji S, Onodera A, et al. (2012) The transcription factor Sox4 is a downstream target of signaling by the cytokine TGF-beta and suppresses T(H)2 differentiation. Nat Immunol 13: 778–786.
44. Yamashita M, Kuwahara M, Suzuki A, Hirahara K, Shinnaksu R, et al. (2008) Bmi1 regulates memory CD4 T cell survival via repression of the Noxa gene. J Exp Med 205: 1109–1120.
45. Suzuki A, Iwamura C, Shinoda K, Tumes DJ, Kimura MY, et al. (2010) Polycomb group gene product Ring1B regulates Th2-driven airway inflammation through the inhibition of Bim-mediated apoptosis of effector Th2 cells in the lung. J Immunol 184: 4510–4520.

nature genetics

Exome sequencing identifies secondary mutations of *SETBP1* and *JAK3* in juvenile myelomonocytic leukemia

Hirotoshi Sakaguchi[1,8], Yusuke Okuno[2,8], Hideki Muramatsu[1,8], Kenichi Yoshida[2,8], Yuichi Shiraishi[3], Mariko Takahashi[2], Ayana Kon[2], Masashi Sanada[2,4], Kenichi Chiba[3], Hiroko Tanaka[5], Hideki Makishima[6], Xinan Wang[1], Yinyan Xu[1], Sayoko Doisaki[1], Asahito Hama[1], Koji Nakanishi[1], Yoshiyuki Takahashi[1], Nao Yoshida[7], Jaroslaw P Maciejewski[6], Satoru Miyano[3,5], Seishi Ogawa[2,4,9] & Seiji Kojima[1,9]

Juvenile myelomonocytic leukemia (JMML) is an intractable pediatric leukemia with poor prognosis[1] whose molecular pathogenesis is poorly understood, except for somatic or germline mutations of RAS pathway genes, including *PTPN11*, *NF1*, *NRAS*, *KRAS* and *CBL*, in the majority of cases[2–4]. To obtain a complete registry of gene mutations in JMML, whole-exome sequencing was performed for paired tumor-normal DNA from 13 individuals with JMML (cases), which was followed by deep sequencing of 8 target genes in 92 tumor samples. JMML was characterized by a paucity of gene mutations (0.85 non-silent mutations per sample) with somatic or germline RAS pathway involvement in 82 cases (89%). The *SETBP1* and *JAK3* genes were among common targets for secondary mutations. Mutations in the latter were often subclonal and may be involved in the progression rather than the initiation of leukemia, and these mutations associated with poor clinical outcome. Our findings provide new insights into the pathogenesis and progression of JMML.

JMML is a rare myelodysplastic/myeloproliferative neoplasm unique to childhood, characterized by excessive proliferation of myelomonocytic cells and hypersensitivity to granulocyte-macrophage colony-stimulating factor[1]. A cardinal genetic feature of JMML is frequent somatic and/or germline mutation of RAS pathway genes, such as *NF1*, *NRAS*, *KRAS*, *PTPN11* and *CBL*, which are mutated in more than 70% of JMML cases in a mutually exclusive manner[2–4]. However, it is still open to question whether RAS pathway mutations are sufficient for the development of JMML or if secondary mutations have a role in the development and progression of this cancer. To address these issues and to better define the molecular pathogenesis of JMML, we performed whole-exome sequencing of paired tumor-normal DNA from 13 cases (**Supplementary Table 1**). We obtained mean coverage in exome sequencing of 137× for tumor samples and 143× for normal samples (**Supplementary Fig. 1**). A Monte-Carlo simulation indicated that the study detected 88% of the existing somatic mutations (Online Methods and **Supplementary Fig. 2**).

Sanger sequencing of 25 candidate non-silent somatic nucleotide alterations confirmed 1 nonsense and 10 missense mutations (**Table 1** and **Supplementary Fig. 3**), with the low true positive rate consistent with the very low numbers of somatic mutations in JMML. Of the 11 somatic mutations, 6 involved known RAS pathway genes. In addition, non-overlapping RAS pathway mutations (6 somatic and 6 germline) were confirmed in 11 of the 13 discovery cases (86%; **Table 1**). For the remaining two cases that lacked documented RAS pathway mutations, we intensively searched for possible germline mutations that could be relevant to the development of JMML. In total, 179 and 167 candidate germline mutations were detected in subjects 77 and 92, respectively, but these mutations did not affect known RAS pathway genes or other cancer-related genes, including the ones registered in the pathway databases (Online Methods). A frameshift deletion in *KMT2D* (also known as *MLL2*; encoding p.Val1670fs) was found in subject 92, who had been diagnosed as having Noonan syndrome on the basis of typical features such as hypertelorism, webbed neck and congenital heart disease (**Supplementary Fig. 3**) but lacked the distinctive facial appearance of Kabuki syndrome, which was shown to be caused by germline *KMT2D* mutations[5].

Five of the 11 somatic mutations were non–RAS pathway mutations, involving *SETBP1* (3 p.Asp868Asn alterations), *JAK3* (1 p.Arg657Gln alteration) and *SH3BP1* (1 p.Ser277Leu alteration), which had not been reported in JMML cases. SETBP1 was originally isolated as a 170-kDa nuclear protein that interacts with SET, a small protein inhibitor of the putative tumor suppressors PP2A and NM23-H1 (ref. 6). Several lines of recent evidence suggest that SETBP1 has a role in leukemogenesis (**Supplementary Fig. 4**)[7–11]. *SETBP1* participates in

[1]Department of Pediatrics, Nagoya University Graduate School of Medicine, Nagoya, Japan. [2]Cancer Genomics Project, Graduate School of Medicine, The University of Tokyo, Tokyo, Japan. [3]Laboratory of DNA Information Analysis, Human Genome Center, Institute of Medical Science, The University of Tokyo, Tokyo, Japan. [4]Department of Pathology and Tumor Biology, Graduate School of Medicine, Kyoto University, Kyoto, Japan. [5]Laboratory of Sequence Analysis, Human Genome Center, Institute of Medical Science, The University of Tokyo, Tokyo, Japan. [6]Department of Translational Hematology and Oncology Research, Taussig Cancer Institute, Cleveland Clinic, Cleveland, Ohio, USA. [7]Department of Hematology and Oncology, Children's Medical Center, Japanese Red Cross Nagoya First Hospital, Nagoya, Japan. [8]These authors contributed equally to this work. [9]These authors jointly directed this work. Correspondence should be addressed to S.O. (sogawa-tky@umin.ac.jp) or S.K. (kojimas@med.nagoya-u.ac.jp).

Received 6 November 2012; accepted 17 June 2013; published online 7 July 2013; doi:10.1038/ng.2698

Table 1 List of gene mutations identified by whole-exome sequencing

	RAS pathway mutations								Other somatic mutations			
	Somatic				Germline							
Subject number	Gene	Change at DNA level	Change at protein level	VAF[a]	Gene	Change at DNA level	Change at protein level	VAF[a]	Gene	Change at DNA level	Change at protein level	VAF[a]
11[b]	*NF1*	c.4537C>T	p.Arg1513*	40.1/24.2	*NF1*	c.5927delG	p.Trp1976fs	44.0/47.1	*SETBP1*	c.2602G>A	p.Asp868Asn	32.6/27.0
63	*KRAS*	c.38G>A	p.Gly13Asp	44.3/0.0	–	–	–	–	–	–	–	–
72	*PTPN11*	c.172A>T	p.Asn58Tyr	48.2/5.7	–	–	–	–	*SETBP1*	c.2602G>A	p.Asp868Asn	45.9/2.5
									JAK3	c.1970G>A	p.Arg657Gln	30.5/2.2
									SH3BP1	c.830C>T	p.Ser277Leu	47.8/5.1
77	–	–	–	–	–	–	–	–	*SETBP1*	c.2602G>A	p.Asp868Asn	33.4/2.1
78	*NRAS*	c.35G>C	p.Gly12Ala	45.5/9.5	–	–	–	–	–	–	–	–
82	–	–	–	–	*CBL*	c.1217del22	p.Thr406fs	34.7/38.9	–	–	–	–
83	–	–	–	–	*NF1*	c.4970A>G	p.Tyr1657Cys	50.0/51.0	–	–	–	–
84	–	–	–	–	*CBL*	c.1096–110del643	p.Glu366_Phe488del	NA/NA	–	–	–	–
85	*PTPN11*	c.226G>A	p.Glu76Lys	47.5/4.4	–	–	–	–	–	–	–	–
86	*KRAS*	c.38G>A	p.Gly13Asp	38.9/3.1	–	–	–	–	–	–	–	–
89[c]	–	–	–	–	*PTPN11*	c.1502T>G	p.Ser502Ala	50.0/49.9	–	–	–	–
91[c]	–	–	–	–	*PTPN11*	c.218C>T	p.Thr73Ile	49.0/48.0	–	–	–	–
92[c]	–	–	–	–	–	–	–	–	–	–	–	–

NA, not available.
[a]Variant allele frequency (VAF) in tumor/reference samples, where the reference was CD3+ T cells, except for subject 63, for whom umbilical cord was used as the reference. [b]Substantial contamination of tumor cell components in the CD3+ T cell reference. [c]Noonan syndrome–associated myeloproliferative disorder.

translocations that result in an aberrant fusion gene (*NUP98-SETBP1*) and overexpression of *SETBP1* in T cell acute lymphoblastic leukemia (T-ALL) and acute myeloid leukemia (AML), respectively[12,13]. *SETBP1* is one of the downstream targets induced by the Evi-1 oncoprotein[14] and, together with *EVI1* and its homolog *PRDM16* (also known as *MEL1*), was reported to be activated through retrovirus integration. SETBP1 is also known to augment the recovery of granulopoiesis after gene therapies for chronic granulomatous disease[15]. *SETBP1* overexpression is found in more than 27% of adult AML cases and is associated with poor survival[13]. The discovery of recurrent hotspot mutations of *SETBP1* provides unequivocal evidence for the leukemogenic role of deregulated SETBP1 function. Notably, the *SETBP1* mutation encoding p.Asp868Asn was identical to one of the *de novo* mutations reported to be causative in Schinzel-Giedion syndrome (SGS; MIM 269150), which is a highly recognizable congenital disease characterized by severe mental retardation, distinctive facial features and

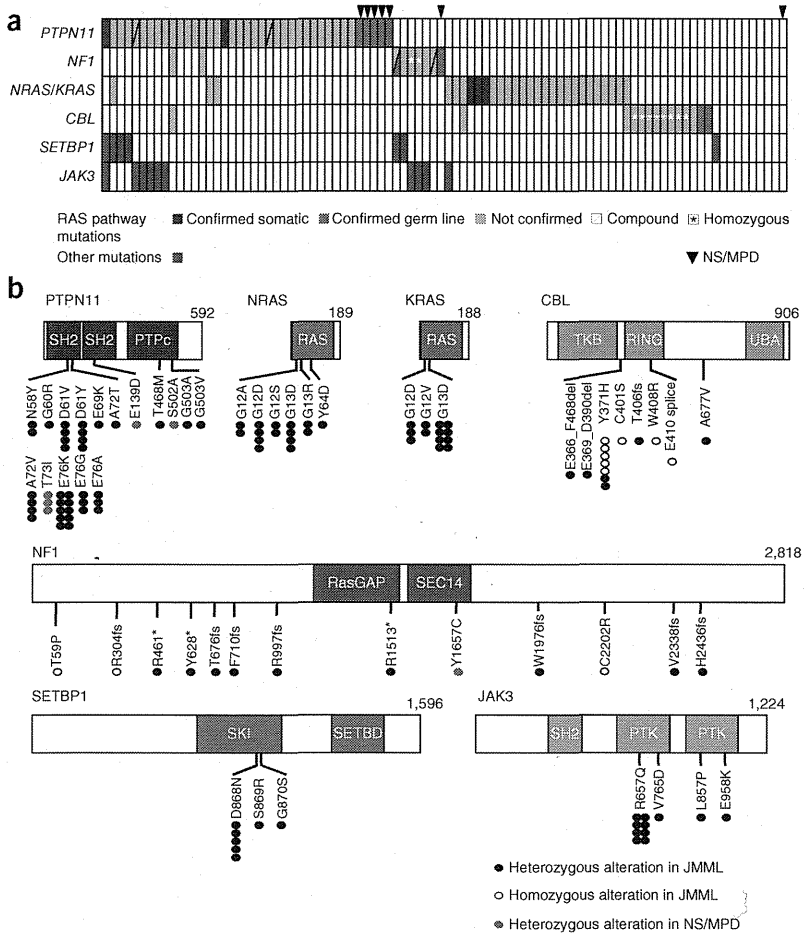

Figure 1 Mutation profiles of 92 JMML cases. (**a**) The mutation status of RAS pathway genes and 2 newly identified gene targets in a cohort of 92 JMML cases is summarized. NS/MPD, Noonan syndrome–associated myeloproliferative disorder. (**b**) The distribution of alterations is shown for each protein. SH2, Src homology 2 domain; PTPc, protein tyrosine phosphatase, catalytic domain; RAS, Ras GTPase family domain; TKB, tyrosine kinase–binding domain; RING, RING-finger domain; UBA, ubiquitin-associated domain; RasGAP, a region of similarity with the catalytic domain of the mammalian p120RasGAP protein in neurofibromin; SEC14, Sec14p-like lipid-binding domain; SKI, v-ski sarcoma viral oncogene homolog domain; SETBD, SET-binding domain; PTK, pseudokinase domain of the protein tyrosine kinases.

Table 2 Subject characteristics

Characteristic	Total cohort (n = 92)	Secondary mutations		P value
		Yes (n = 16)	No (n = 76)	
Sex (male/female)	61/31	12/4	49/27	NS
Median age at diagnosis in months (range)	19 (1–160)	38 (2–160)	13 (1–79)	<0.001
Diagnosis				
JMML	85	16	69	
NS/MPD	7	0	7	
Genetic mutations in RAS pathway				
PTPN11	39	9	30	NS
NF1	9	5	4	0.001
RAS (*NRAS* or *KRAS*)	28 (15/13)	2 (1/1)	26 (14/12)	0.08
CBL	14	0	14	0.06
Without RAS pathway mutation	10	1	9	NS
Secondary genetic mutations				
SETBP1	7	7	0	
JAK3	10	10	0	
Cytogenetics				
Normal karyotype	77	12	65	NS
Monosomy 7	8	1	7	NS
Trisomy 8	4	2	2	NS
Other abnormalities	3	1	2	NS
WBC count at diagnosis $\times 10^9$/l, median (range)	30.0 (1.0–563)	29.6 (5.6–563)	30.0 (1.0–131)	NS
Monocyte count at diagnosis $\times 10^9$/l, median (range)	4.6 (0.2–31.6)	3.1 (0.5–15.2)	4.9 (0.2–31.6)	NS
Percent HbF at diagnosis, median (range)	21 (0–68)	26 (9–55)	16 (0–68)	NS
PLT at diagnosis $\times 10^9$/l, median (range)	61.0 (1.4–483)	47.5 (1.4–175)	65.0 (5.0–483)	NS
HSCT (+/–)	56/36	16/0	40/36	
Alive/deceased	62/30	7/9	55/21	
Percent probability of 5-year overall survival (95% CI)	60 (46–71)	33 (10–59)	65 (49–77)	0.10
Percent probability of 5-year transplantation-free survival (95% CI)	15 (6–27)	0 (0–0)	18 (8–33)	0.007

JMML, juvenile myelomonocytic leukemia; NS/MPD, Noonan syndrome–associated myeloproliferative disorder; WBC, white blood cell; HbF, hemoglobin F; HSCT, hematopoietic stem cell transplantation; NS, not significant. We compared the difference between the subjects with and without secondary mutation, and P values were calculated by two-sided Fisher's exact test or Mann-Whitney U test.

multiple congenital malformations. Individuals with SGS with this mutation have a higher than normal prevalence of tumors, including of neuroepithelial neoplasia[16], although development of myeloid malignancies has not been reported so far.

To further validate our findings, we screened the entire cohort of 92 JMML cases for gene mutations in the newly identified 3 genes together with known RAS pathway targets using deep sequencing[17] (**Supplementary Fig. 5**).

RAS pathway mutations were found in 82 of 92 cases (89%) in a mutually exclusive manner, with *PTPN11* mutations predominant, followed by *NRAS*, *KRAS*, *CBL* and *NF1* mutations (**Fig. 1a** and **Table 2**). In accordance with previous reports, most of the *CBL* (8/14) and *NF1* (4/9) mutations were biallelic (**Fig. 1a,b** and **Supplementary Table 2**)[2,3,18], whereas the majority of mutations in *PTPN11*, *NRAS* and *KRAS* were heterozygous[4]. The individuals without RAS pathway mutations (n = 10) were vigorously investigated by whole-genome sequencing of tumor-normal paired samples (n = 2; **Supplementary Fig. 6**) or by whole-exome sequencing of only tumor samples (n = 8; **Supplementary Fig. 7**). As anticipated, we found no known RAS pathway mutations.

On the other hand, 18 mutations were found in *SETBP1* (n = 7) or *JAK3* (n = 11) in 16 cases (**Fig. 1a,b**, **Table 2** and **Supplementary Table 2**), with these mutations more frequent in cases with mutated *PTPN11* (and possibly *NF1*) than in cases with mutated *NRAS*, *KRAS*

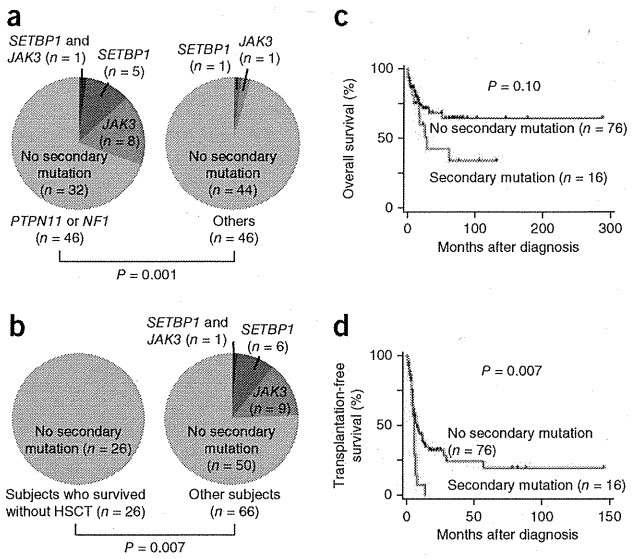

Figure 2 Clinical features of JMML cases with or without secondary mutations. (**a**,**b**) Frequency of secondary mutations in individuals with JMML depending on the type of RAS pathway mutations (left, *PTPN11* or *NF1*; right, other or no mutations) (**a**) and the status of HSCT (**b**). P values were calculated by two-sided Fisher's exact test. (**c**,**d**) The impact of secondary mutations on overall (**c**) and transplantation-free (**d**) survival is shown in Kaplan-Meier survival curves, where statistical significance was tested by log-rank test.

or *CBL* (**Fig. 2a**). Mutations in *SH3BP1*, encoding SH3 domain–binding protein 1, were not recurrent. All *SETBP1* mutations were heterozygous and occurred within the portion of the gene encoding the SKI domain, with six identical to the *de novo* recurrent mutations reported in SGS and five identical to the mutation encoding the p.Asp868Asn alteration (**Fig. 1b**). RT-PCR analysis showed that the wild-type and mutant alleles of *SETBP1* were equally expressed (**Supplementary Fig. 8**). Similarly, 8 of the 11 *JAK3* mutations in 10 cases were the well-described activating mutation (encoding a p.Arg657Gln alteration) found in various hematological malignancies, including Down syndrome–associated acute megakaryoblastic leukemia[19–23], ALL[24,25] and natural killer (NK)/T cell lymphoma[26], and the remaining 3 were also within the portions of the gene encoding the pseudokinase or kinase domain, suggestive of gain of function.

Deep sequencing of the relevant mutant alleles enabled an accurate estimation of allele frequencies for individual mutations (**Supplementary Fig. 9**). *SETBP1* and *JAK3* mutations showed lower allele frequencies (but not with statistical significance for *SETBP1*) than did the corresponding RAS pathway mutations (**Supplementary Fig. 10a**), indicating that the former mutations represent secondary genetic hits that contributed to clonal evolution after the main tumor population was established (**Supplementary Fig. 10b**). Individuals with secondary mutations had shorter lengths of survival compared to those without mutations: 5-year overall survival (hazards ratio (HR) = 1.90, 95% CI = 0.87–4.19). In addition, none of the individuals with JMML who survived without hematopoietic stem cell transplantation (HSCT; $n = 26$) harbored any of the secondary mutations, and individuals with secondary mutations showed significantly inferior 5-year transplant-free survival (HR = 2.18, 95% CI = 1.18–4.02) (**Fig. 2b–d** and **Table 2**).

JMML is characterized by a paucity of gene mutations. The average number of mutations per sample (0.85; range of 0–4) was unexpectedly low compared to those reported in other human cancers (**Supplementary Fig. 11**); excluding common RAS pathway mutations, only 5 mutations were detected in 3 of the 13 discovery cases. This small number of mutations is only comparable to the figure reported for retinoblastoma (mean of 3.3 per case; range of 0–5) (ref. 27) and is in stark contrast to the abundance of gene mutations in chronic myelomonocytic leukemia (CMML) in adult cases, where the mean number of non-silent mutations was 12.4 per sample, of which 3.1 represented known driver changes (ref. 17 and K.Y., M.S., Y.S., D. Nowak, Y. Nagata *et al.*, unpublished data), underscoring the distinct pathogenesis in these two neoplasms that show indistinguishable morphology. The impact of germline events is underscored by the fact that 6 of the 13 discovery cases harbored germline RAS pathway mutations and an additional case without known RAS pathway mutations showed constitutive abnormalities similar to Noonan syndrome. Despite the central role of RAS pathway mutations, a small subset of cases had no documented RAS pathway mutations, even after whole-exome analysis in the two RAS pathway mutation–negative cases, raising the possibility that the latter cases represent a genetically distinct myeloproliferative neoplasm in childhood.

Another key finding in the current study is the discovery of secondary mutations that involve *SETBP1* and *JAK3*. Detected only in a subpopulation of leukemic cells, most of these mutations are thought to be involved in the progression rather than the establishment of JMML and were associated with poor clinical outcome. *SETBP1* is a newly identified proto-oncogene, and identical mutations in this gene have recently been reported in 15–25% of adult cases with atypical chronic myeloid leukemia (CML)[10], CMML and secondary AML[28]. Affecting one of three highly conserved amino acid positions, *SETBP1* mutations have been shown to abolish the binding of an E3 ubiquitin ligase (β-TrCP1) to SETBP1, which prevents ubiquitination and subsequent degradation, leading to gain of function through the consequent increase in SETBP1 protein amounts[10,28]. Although the precise leukemogenic mechanisms of *SETBP1* mutations are still unclear, we have shown that mutant *SETBP1* alleles confer self-renewal capability to myeloid progenitors *in vitro*, and *SETBP1* mutations in adult leukemia were associated with increases in *HOXA9* and *HOXA10* expression[28]. Recurrent *JAK3* mutations in JMML are also noteworthy. The JAK-STAT pathway is a key component of normal hematopoiesis[29]. As in other hematopoietic malignancies[20], the p.Arg657Gln alteration represents the most frequent change in JMML. This alteration confers interleukin (IL)-3 independence to Ba/F3 cells and induces STAT5 phosphorylation[20]. Targeting the JAK-STAT pathway with a pan-JAK inhibitor such as CP-690550 (ref. 30) could be a promising therapeutic possibility for patients with *JAK3*-mutated JMML.

In conclusion, our whole-exome sequencing analysis identified the spectrum of gene mutations in JMML. Together with the high frequency of RAS pathway mutations, the paucity of non–RAS pathway mutations is a prominent feature of JMML. Mutations of *SETBP1* and *JAK3* were common recurrent secondary events presumed to be involved in tumor progression and were associated with poor clinical outcomes. Our findings provide an important clue to understanding the pathogenesis of JMML that may help in the development of novel diagnostics and therapeutics for this leukemia.

URLs. Genomon, http://genomon.hgc.jp/exome/en/; BioCarta, http://www.biocarta.com/; dbSNP131, http://www.ncbi.nlm.nih.gov/projects/SNP/; RefSeq database, http://www.ncbi.nlm.nih.gov/RefSeq/.

METHODS

Methods and any associated references are available in the online version of the paper.

Accession code. We deposited whole-genome and whole-exome sequence data in the European Genome-phenome Archive under accession EGAS00001000521.

Note: Supplementary information is available in the online version of the paper.

ACKNOWLEDGMENTS

We thank the subjects and their parents for participating in this study. This work was supported by the Research on Measures for Intractable Diseases Project from the Ministry of Health, Labor and Welfare, by Grants-in-Aid from the Ministry of Health, Labor and Welfare of Japan and KAKENHI (23249052, 22134006 and 21790907), by the Project for the Development of Innovative Research on Cancer Therapeutics (P-DIRECT) and by the Japan Society for the Promotion of Science through the Funding Program for World-Leading Innovative R&D on Science and Technology.

AUTHOR CONTRIBUTIONS

H.S., Y.O., H. Muramatsu, K.Y., M.T., A.K. and M.S. designed and performed the research, analyzed the data and wrote the manuscript. Y.S., K.C., H.T. and S.M. performed bioinformatics analyses of the resequencing data. X.W. and Y.X. performed Sanger sequencing. S.D., A.H., K.N., Y.T. and N.Y. collected specimens and performed the research. H. Makishima and J.P.M. designed the research and analyzed the data. S.O. and S.K. led the entire project and wrote the manuscript.

COMPETING FINANCIAL INTERESTS

The authors declare no competing financial interests.

1. Pinkel, D. *et al.* Differentiating juvenile myelomonocytic leukemia from infectious disease. *Blood* **91**, 365–367 (1998).
2. Loh, M.L. *et al.* Mutations in *CBL* occur frequently in juvenile myelomonocytic leukemia. *Blood* **114**, 1859–1863 (2009).
3. Muramatsu, H. *et al.* Mutations of an E3 ubiquitin ligase c-*Cbl* but not *TET2* mutations are pathogenic in juvenile myelomonocytic leukemia. *Blood* **115**, 1969–1975 (2010).
4. Pérez, B. *et al.* Genetic typing of *CBL*, *ASXL1*, *RUNX1*, *TET2* and *JAK2* in juvenile myelomonocytic leukaemia reveals a genetic profile distinct from chronic myelomonocytic leukaemia. *Br. J. Haematol.* **151**, 460–468 (2010).
5. Ng, S.B. *et al.* Exome sequencing identifies *MLL2* mutations as a cause of Kabuki syndrome. *Nat. Genet.* **42**, 790–793 (2010).
6. Minakuchi, M. *et al.* Identification and characterization of SEB, a novel protein that binds to the acute undifferentiated leukemia–associated protein SET. *Eur. J. Biochem.* **268**, 1340–1351 (2001).
7. Damm, F. *et al. SETBP1* mutations in 658 patients with myelodysplastic syndromes, chronic myelomonocytic leukemia and secondary acute myeloid leukemias. *Leukemia* **27**, 401–403 (2013).
8. Laborde, R.R. *et al. SETBP1* mutations in 415 patients with primary myelofibrosis or chronic myelomonocytic leukemia: independent prognostic impact in CMML. *Leukemia* published online; doi:10.1038/leu.2013.97 (5 April 2013).
9. Meggendorfer, M. *et al. SETBP1* mutations occur in 9% of MDS/MPN and in 4% of MPN cases and are strongly associated with atypical CML, monosomy 7, isochromosome i(17)(q10), *ASXL1* and *CBL* mutations. *Leukemia* published online; doi:10.1038/leu.2013.133 (30 April 2013).
10. Piazza, R. *et al.* Recurrent *SETBP1* mutations in atypical chronic myeloid leukemia. *Nat. Genet.* **45**, 18–24 (2013).
11. Thol, F. *et al. SETBP1* mutation analysis in 944 patients with MDS and AML. *Leukemia* published online; doi:10.1038/leu.2013.145 (7 May 2013).
12. Panagopoulos, I. *et al.* Fusion of *NUP98* and the SET binding protein 1 (*SETBP1*) gene in a paediatric acute T cell lymphoblastic leukaemia with t(11;18)(p15;q12). *Br. J. Haematol.* **136**, 294–296 (2007).
13. Cristóbal, I. *et al.* SETBP1 overexpression is a novel leukemogenic mechanism that predicts adverse outcome in elderly patients with acute myeloid leukemia. *Blood* **115**, 615–625 (2010).
14. Goyama, S. *et al.* Evi-1 is a critical regulator for hematopoietic stem cells and transformed leukemic cells. *Cell Stem Cell* **3**, 207–220 (2008).
15. Ott, M.G. *et al.* Correction of X-linked chronic granulomatous disease by gene therapy, augmented by insertional activation of *MDS1-EVI1*, *PRDM16* or *SETBP1*. *Nat. Med.* **12**, 401–409 (2006).
16. Hoischen, A. *et al. De novo* mutations of *SETBP1* cause Schinzel-Giedion syndrome. *Nat. Genet.* **42**, 483–485 (2010).
17. Yoshida, K. *et al.* Frequent pathway mutations of splicing machinery in myelodysplasia. *Nature* **478**, 64–69 (2011).
18. Flotho, C. *et al.* Genome-wide single-nucleotide polymorphism analysis in juvenile myelomonocytic leukemia identifies uniparental disomy surrounding the *NF1* locus in cases associated with neurofibromatosis but not in cases with mutant *RAS* or *PTPN11*. *Oncogene* **26**, 5816–5821 (2007).
19. Walters, D.K. *et al.* Activating alleles of *JAK3* in acute megakaryoblastic leukemia. *Cancer Cell* **10**, 65–75 (2006).
20. Sato, T. *et al.* Functional analysis of *JAK3* mutations in transient myeloproliferative disorder and acute megakaryoblastic leukaemia accompanying Down syndrome. *Br. J. Haematol.* **141**, 681–688 (2008).
21. De Vita, S. *et al.* Loss-of-function *JAK3* mutations in TMD and AMKL of Down syndrome. *Br. J. Haematol.* **137**, 337–341 (2007).
22. Norton, A. *et al.* Analysis of *JAK3*, *JAK2*, and *C-MPL* mutations in transient myeloproliferative disorder and myeloid leukemia of Down syndrome blasts in children with Down syndrome. *Blood* **110**, 1077–1079 (2007).
23. Kiyoi, H., Yamaji, S., Kojima, S. & Naoe, T. *JAK3* mutations occur in acute megakaryoblastic leukemia both in Down syndrome children and non–Down syndrome adults. *Leukemia* **21**, 574–576 (2007).
24. Elliott, N.E. *et al.* FERM domain mutations induce gain of function in JAK3 in adult T-cell leukemia/lymphoma. *Blood* **118**, 3911–3921 (2011).
25. Zhang, J. *et al.* The genetic basis of early T-cell precursor acute lymphoblastic leukaemia. *Nature* **481**, 157–163 (2012).
26. Koo, G.C. *et al.* Janus kinase 3–activating mutations identified in natural killer/T-cell Lymphoma. *Cancer Discov.* **2**, 591–597 (2012).
27. Zhang, J. *et al.* A novel retinoblastoma therapy from genomic and epigenetic analyses. *Nature* **481**, 329–334 (2012).
28. Makishima, H. *et al.* Somatic *SETBP1* mutations in myeloid malignancies. *Nat. Genet.* published online; doi:10.1038/ng.2696 (7 July 2013).
29. Crozatier, M. & Meister, M. *Drosophila* haematopoiesis. *Cell. Microbiol.* **9**, 1117–1126 (2007).
30. Changelian, P.S. *et al.* Prevention of organ allograft rejection by a specific Janus kinase 3 inhibitor. *Science* **302**, 875–878 (2003).

ONLINE METHODS

Subjects. We studied 92 children (61 boys and 31 girls) with JMML, including 7 individuals with NS/MPD, who were diagnosed as having JMML in institutions throughout Japan. Written informed consent was obtained from subjects' parents before sample collection. This study was approved by the ethics committees of the Nagoya University Graduate School of Medicine and the University of Tokyo in accordance with the Declaration of Helsinki. Diagnosis with JMML was made on the basis of internationally accepted criteria[1]. Characteristics of the 92 JMML cases are summarized in **Table 2**. The median age at diagnosis was 16 months (range of 1–160 months). Karyotypic abnormalities were detected in 16 subjects, including in 8 with monosomy 7. Fifty-six of the 92 subjects (61%) received allogeneic HSCT.

Sample preparation. Genomic DNA was extracted using the QIAamp DNA Blood Mini kit and the QIAamp DNA Investigator kit (Qiagen) according to the manufacturer's instructions. The T Cell Activation/Expansion kit, human (Miltenyi Biotec) was used for the expansion of $CD3^+$ T cells from subjects' peripheral blood or bone marrow mononuclear cells[3].

Whole-exome sequencing. Exome capture from paired tumor-reference DNA was performed using SureSelect Human All Exon V3 (Agilent Technologies), covering 50 Mb of coding exons, according to the manufacturer's protocol. Enriched exome fragments were subjected to massively parallel sequencing using the HiSeq 2000 platform (Illumina). Candidate somatic mutations were detected through our in-house pipeline (Genomon) as previously described[17].

Detection of mutations from whole-exome sequencing data. Detection of candidate somatic mutations was performed according to previously described algorithms with minor modifications[17]. Briefly, the number of reads containing single-nucleotide variations (SNVs) and indels in both tumor and reference samples was determined using SAMtools[31], and the null hypothesis of equal allele frequencies in tumor and reference samples was tested using the two-tailed Fisher's exact test. A variant was adopted as a candidate somatic mutation if it had $P < 0.01$, if it was observed in bidirectional reads (in both plus and minus strands of the reference sequence) and if its allele frequency was less than 0.25 in the corresponding reference sample. For the detection of germline mutations in RAS pathway genes, SNVs and indels having allele frequencies of more than 0.25 (SNVs) and 0.10 (indels) were interrogated for 46 genes, which consisted of known JMML-related RAS pathway genes and genes registered in the pathway databases ('Ras signaling pathway' in BioCarta and 'signaling to RAS' in Reactome[32]). For variant calls in tumor samples for which the paired normal reference was not available, candidate variants in the RAS pathway were detected at an allele frequency of >0.10. Finally, the list of candidate somatic and/or germline mutations was generated by excluding synonymous SNVs and other variants registered in either dbSNP131 or an in-house SNP database constructed from 180 individual samples. All candidates were validated by Sanger sequencing as previously described.

Estimation of tumor content. The tumor content of bone marrow specimens was estimated from the allele frequency of the somatic mutations identified by deep sequencing. For homozygous mutations, as indicated by an allele frequency of >0.75, the tumor content (F_{tumor}) was calculated from the observed frequency ($F_{observed}$) of the mutation according to the following equation: $F_{tumor} = 2 \times F_{observed} - 1$. For heterozygous mutations, the tumor content was calculated by doubling the allele frequency.

Power analysis of whole-exome sequencing. The power of detecting somatic mutations at each nucleotide position in whole-exome sequencing was estimated by Monte-Carlo simulation ($n = 1{,}000$) on the basis of the observed mean depth of coverage for each exon in germline and tumor samples and the observed tumor content for each sample, which were estimated using the allele frequencies of the observed mutations. For the samples with no observed somatic mutations, the average tumor content of the informative samples was employed. Simulations were performed across a total of 192,424 exons.

Copy number analysis in whole-exome sequencing data. To detect copy number lesions at a single-exon level, the mean coverage of each exon normalized by the mean depth of coverage of the entire sample was compared with that of 12 unrelated normal DNA samples. Exons showing normalized coverage greater than 3 s.d. from the mean coverage of the reference samples were called as candidates for copy number alterations. All candidate exons of RAS pathway genes were visually inspected using the Integrative Genomics Viewer[33] and were validated by Sanger sequencing of corresponding putative breakpoint-containing fragments.

Targeted deep sequencing. Deep sequencing of the targeted genes was performed essentially as described in the 'deep sequencing of pooled target exons' section in ref. 17, except that target DNA was not pooled. Briefly, all exons of *PTPN11*, *NF1*, *KRAS*, *NRAS*, *CBL*, *SETBP1*, *JAK3* and *SH3BP1* were PCR amplified with Quick Taq HS DyeMix (TOYOBO) and the PrimeSTAR GXL DNA Polymerase kit (Takara Bio) using primers including the NotI restriction site (**Supplementary Table 3**). The PCR products from an individual sample were combined and purified with the QIAquick PCR Purification kit (Qiagen) for subsequent digestion with NotI (Fermentas). Digested PCR product was purified, concatenated with T4 DNA ligase (Takara Bio) and sonicated to generate fragments with an average size of 150 bp using Covaris. Fragments were processed for sequencing according to a modified Illumina paired-end library protocol, and sequences were read by a HiSeq 2000 instrument using a 100-bp paired-end read protocol.

Variant calls in targeted deep sequencing. Data processing and variant calling were performed with modifications to the protocol described in a previous publication[17]. Each read was aligned to the set of targeted sequences from PCR amplification, with BLAT[34] instead of Burrows-Wheeler Aligner (BWA)[35] used with the -fine option. Mapping information in the .psl format was converted to the .sam format with paired-read information. Of the successfully mapped reads, reads were excluded from further analysis if they mapped to multiple sites, mapped with more than four mismatched bases or had more than ten soft-clipped bases. Next, the Estimation_CRME script was run to eliminate strand-specific errors and exclude PCR-derived errors. A strand-specific mismatch ratio was calculated for each nucleotide variant for both strands using the bases from read cycles 11 to 50 on the next-generation sequencer. By excluding the top five cycles showing the highest mismatch rates, strand-specific mismatch rates were recalculated, and the smaller value between both strands was adopted as a nominal mismatch ratio for that variant. After excluding variants found in dbSNP131 or the in-house SNP database, non-silent variants having a mismatch ratio of greater than 0.05 were called as candidates, unless they had median values of the mismatch ratio at the relevant nucleotide positions in the 92 samples of greater than 0.01, as such variants were likely to be caused by systematic PCR problems. Finally, candidates with mismatch ratios of >0.15 were further validated by Sanger sequencing.

Annotation of the detected mutations. Detected mutations were annotated using ANNOVAR[36]. The positions of the mutations were based on the following RefSeq transcript sequences: NM_002834.3 for *PTPN11*, NM_000267.3 for *NF1*, NM_002524.4 for *NRAS*, NM_004985.3 for *KRAS*, NM_005188.3 for *CBL*, NM_015559.2 for *SETBP1* and NM_000215.3 for *JAK3*. The effect of the mutations on protein function was assessed by SIFT[37], PolyPhen-2 (ref. 38) and MutationTaster[39].

Whole-genome sequencing. Paired tumor-reference DNA samples were sequenced with the HiSeq 2000 platform according to the manufacturer's instructions to obtain 30× read coverage for reference samples and 40× coverage for tumor samples. Obtained FASTQ sequences were aligned to the human reference genome (hg19) using BWA[35] 0.5.8 with default parameters. Alignment of pairs of sequences, at least one of which was not mapped or was considered to have possible mapping problems (with mapping quality of less than 40, insertions or deletions, soft-clipped sequence of more than 10% of the length of the original sequence, irregular paired-read orientation or mate distance of greater than 2,000 bp), was attempted with BLAT[34] using default parameters, except for stepSize = 5 and repMatch = 2,253. Mapping statistics were calculated by counting the bases at each genomic position with SAMtools[31]. For variant calling, variant and reference bases with base quality of >30 were counted in both germline and tumor samples, and the Fisher's

exact test was applied. Variants with P of <0.01 were called. Variants having allele frequency of >0.25 in the germline sample were excluded. Variants found in 12 unrelated germline samples with an allele frequency of >0.01 on average were also excluded owing to the high probability that they represented false positive calls. Copy number estimation was performed by calculating the averaged ratio of read depths in germline and tumor samples in 10,000-base bins. An allele-specific copy number plot was generated by measuring the allele frequency of the tumor sample at the positions in which more than 25% of the allele mismatch was observed in germline samples. For the detection of chromosomal structural variations, soft-clipped sequences that could be mapped to a unique genomic position were selected. Structural variation candidates that had more than four supporting read pairs in total and at least one read pair from each side of the breakpoint were called. Contig sequences were generated by assembling the reads within 200 bp of the breakpoint with CAP3 (ref. 40), and structural variations having the contig sequence that could be aligned to the alternate assembly of the hg19 genome with more than 93% identity were excluded as false positives. Structural variations with read depth of greater than 150 on at least one side of the breakpoint were considered to be mapped to a repeat element and were also excluded. For detection of viruses, unmapped sequences were aligned to the collection of all viral genomes in the RefSeq database using BLAT. A virus was considered to be detected if its genome was covered by mean read coverage of >1.

cDNA sequencing. Total RNA was extracted using the RNeasy Mini kit (Qiagen) and was reverse transcribed with the ThermoScript RT-PCR system (Life Technologies). Target sequences were PCR amplified with the PrimeSTAR GXL DNA Polymerase kit using the primers listed in **Supplementary Table 3** and were sequenced.

Statistical analysis. For comparison of the frequency of mutations or other clinical features between disease groups, categorical variables were analyzed using the Fisher's exact test, and continuous variables were tested using the Mann-Whitney U test. Overall survival and transplantation-free survival were estimated by the Kaplan-Meier method. Hazard ratios for survival with 95% CIs were estimated according to the Cox proportional hazards model, and difference in survival was tested by log-rank test. STATA version 12.0 (StataCorp) was used for all statistical calculations.

31. Li, H. *et al.* The Sequence Alignment/Map format and SAMtools. *Bioinformatics* **25**, 2078–2079 (2009).
32. Matthews, L. *et al.* Reactome knowledgebase of human biological pathways and processes. *Nucleic Acids Res.* **37**, D619–D622 (2009).
33. Thorvaldsdóttir, H., Robinson, J.T. & Mesirov, J.P. Integrative Genomics Viewer (IGV): high-performance genomics data visualization and exploration. *Brief. Bioinform.* **14**, 178–192 (2013).
34. Kent, W.J. BLAT—the BLAST-like alignment tool. *Genome Res.* **12**, 656–664 (2002).
35. Li, H. & Durbin, R. Fast and accurate short read alignment with Burrows-Wheeler transform. *Bioinformatics* **25**, 1754–1760 (2009).
36. Wang, K., Li, M. & Hakonarson, H. ANNOVAR: functional annotation of genetic variants from high-throughput sequencing data. *Nucleic Acids Res.* **38**, e164 (2010).
37. Kumar, P., Henikoff, S. & Ng, P.C. Predicting the effects of coding non-synonymous variants on protein function using the SIFT algorithm. *Nat. Protoc.* **4**, 1073–1081 (2009).
38. Adzhubei, I.A. *et al.* A method and server for predicting damaging missense mutations. *Nat. Methods* **7**, 248–249 (2010).
39. Schwarz, J.M., Rödelsperger, C., Schuelke, M. & Seelow, D. MutationTaster evaluates disease-causing potential of sequence alterations. *Nat. Methods* **7**, 575–576 (2010).
40. Huang, X. & Madan, A. CAP3: A DNA sequence assembly program. *Genome Res.* **9**, 868–877 (1999).

Pediatr Blood Cancer 2013;60:836–841

Wiskott–Aldrich Syndrome Presenting With a Clinical Picture Mimicking Juvenile Myelomonocytic Leukaemia

Ayami Yoshimi, MD,[1]* Yoshiro Kamachi, MD,[2] Kosuke Imai, MD,[3] Nobuhiro Watanabe, MD,[4] Hisaya Nakadate, MD,[5] Takashi Kanazawa, MD,[6] Shuichi Ozono, MD,[7] Ryoji Kobayashi, MD,[8] Misa Yoshida, MD,[9] Chie Kobayashi, MD,[10] Asahito Hama, MD,[2] Hideki Muramatsu, MD,[2] Yoji Sasahara, MD,[11] Marcus Jakob, MD,[12] Tomohiro Morio, MD,[13] Stephan Ehl, MD,[14] Atsushi Manabe, MD,[15] Charlotte Niemeyer, MD,[1] and Seiji Kojima, MD[2]

Background. Wiskott–Aldrich syndrome (WAS) is a rare X-linked immunodeficiency caused by defects of the WAS protein (*WASP*) gene. Patients with WAS typically demonstrate micro-thrombocytopenia. ***Procedures.*** The report describes seven male infants with WAS that initially presented with leukocytosis, monocytosis, and myeloid and erythroid precursors in the peripheral blood (PB) and dysplasia in the bone marrow (BM), which was initially indistinguishable from juvenile myelomonocytic leukaemia (JMML). ***Results.*** The median age of affected patients was 1 month (range, 1–4 months). Splenomegaly was absent in four of these patients, which was unusual for JMML. A mutation analysis of genes in the RAS-signalling pathway did not support a diagnosis of JMML. Non-haematological features, such as eczema (n = 7) and bloody stools (n = 6), ultimately led to the diagnosis of WAS at a median age of 4 months (range, 3–8 months), which was confirmed by absent (n = 6) or reduced (n = 1) WASP expression in lymphocytes by flow cytometry (FCM) and a *WASP* gene mutation. Interestingly, mean platelet volume (MPV) was normal in three of five patients and six of seven patients demonstrated occasional giant platelets, which was not compatible with WAS. ***Conclusions.*** These data suggest that WAS should be considered in male infants presenting with JMML-like features if no molecular markers of JMML can be detected. Pediatr Blood Cancer 2013;60:836–841.

Key words: children; juvenile myelomonocytic leukaemia; Wiskott–Aldrich syndrome

INTRODUCTION

Wiskott–Aldrich syndrome (WAS) is a rare X-linked recessive disorder, characterized by micro-thrombocytopenia, eczematous skin disease, and recurrent infections. The incidence of WAS is 1–10 in 1 million male new-borns. Affected patients have a predisposition to autoimmune diseases and lymphoid malignancies [1,2]. The responsible gene is *WASP*, which encodes the 502 amino acid WASP protein [3]. WASP is expressed selectively in hematopoietic cells and is involved in cell signalling and cytoskeleton reorganization [3]. Specific types of defects in WASP are often but not invariably associated with the severity of disease and clinical phenotype. Lack of WASP expression causes the most severe phenotype (i.e., classic WAS), whereas inactivating *WASP* missense mutations allow residual protein expression and can cause less severe X-linked thrombocytopenia (XLT) [4,5]. Gain-of-function mutations generate X-linked neutropenia (XLN) [6,7].

Juvenile myelomonocytic leukaemia (JMML) is a rare disease in children that occurs with an estimated incidence of 1–2 cases per million [8]. JMML has characteristics of both myelodysplastic syndrome (MDS) and myeloproliferative disorders (MPD) and is categorized in the MDS/MPD category in the World Health Organization (WHO) classification [9–11]. Clinical and haematological manifestations of JMML include hepatosplenomegaly, skin rash, lymphadenopathy, leukoerythroblastosis, monocytosis, and thrombocytopenia. Recent studies show that deregulated activation of the RAS/MAPK signalling pathway plays a central role in the pathogenesis of JMML. Gene mutations in either the *RAS*, *PTPN11*, *NF1*, or *CBL* genes involved in this pathway are detected in about 80% of JMML patients [12–18].

Micro-thrombocytopenia is the key haematological finding in patients with WAS. However, myelopoiesis and erythropoiesis are usually not affected, despite the fact that WASP is expressed in various hematopoietic cells [19]. The present report describes seven cases of male infants with classical WAS who demonstrated haematological abnormalities mimicking JMML. Importantly, patients can present with JMML-like features before the full clinical manifestations of WAS become apparent. Moreover, nor-

[1]Department of Paediatrics and Adolescent Medicine, University of Freiburg, Freiburg, Germany; [2]Department of Paediatrics, Nagoya University Graduate School of Medicine, Nagoya, Japan; [3]Department of Paediatrics, Perinatal and Maternal Medicine, Tokyo Medical and Dental University, Tokyo, Japan; [4]Division of Haematology and Oncology, Children's Medical Center, Japanese Red Cross Nagoya First Hospital, Nagoya, Japan; [5]Department of Paediatrics, Kitasato University School of Medicine, Sagamihara, Japan; [6]Department of Paediatrics and Developmental Medicine, Gunma University Graduate School of Medicine, Gunma, Japan; [7]Department of Paediatrics and Child Health, Kurume University School of Medicine, Kurume, Japan; [8]Department of Paediatrics, Sapporo Hokuyu Hospital, Sapporo, Japan; [9]Division of Haemato-Oncology/Regeneration Medicine, Kanagawa Children's Medical Center, Kanagawa, Japan; [10]Department of Paediatrics, University of Tsukuba, Tsukuba, Japan; [11]Department of Paediatrics, Tohoku University Graduate School of Medicine, Sendai, Japan; [12]Department of Paediatrics and Adolescent Medicine, University of Regensburg, Regensburg, Germany; [13]Department of Paediatrics and Developmental Biology, Tokyo Medical and Dental University Graduate School of Medical and Dental Sciences, Tokyo, Japan; [14]Centre of Chronic Immunodeficiency, University of Freiburg, Freiburg, Germany; [15]Department of Paediatrics, St. Luke's International Hospital, Tokyo, Japan

Grant sponsor: Ministry of Health, Labour, and Welfare of Japan, Tokyo.

Conflict of interest: Nothing to report.

*Correspondence to: Ayami Yoshimi, MD, PhD, Department of Paediatrics and Adolescent Medicine, Paediatric Haematology and Oncology, University of Freiburg, Mathildenstrasse 1, 79106 Freiburg, Germany. E-mail: ayami.yoshimi@uniklinik-freiburg.de

Received 22 July 2012; Accepted 11 September 2012

DOI 10.1002/pbc.24359
Published online 28 September 2012 in Wiley Online Library (wileyonlinelibrary.com).

mal mean platelet volume (MPV) and the presence of the giant platelets complicated the diagnostic evaluation in some of our patients.

PATIENTS AND METHODS

Patients

In 2007, we described a case of a male patient (patient #1) with WAS who demonstrated JMML-like clinical features [20]. Briefly, thrombocytopenia was detected shortly after birth. He suffered from bloody diarrhoea from the age of 9 days. At the age of 42 days, leukocytosis with myeloid/erythroid precursors and monocytosis was detected. Bone marrow (BM) aspirates showed hypercellularity with significant predominance of myelopoiesis and dysplastic features. The morphological features were compatible with JMML. Subsequently, the white blood cell (WBC) count increased to 52.0×10^9/L with the appearance of peripheral blasts (3%) and persistent fever. Intravenous administration of various antibiotics had no effect on fever and leukocytosis. Oral 6-mercaptopurine (6-MP) was administered, which resulted in disappearance of leukocytosis. Positive results of cytomegalovirus (CMV)-IgM/IgG and a low level pp65 CMV-antigen (Ag) cells were transitionally noted without CMV-related symptoms. Intravenous administration of ganciclovir (GCV) led to the elimination of CMV-Ag but not to any improvement of JMML-like features. At the age of 7 months, mild atopic dermatitis-like eczema was recognized, which finally led to the clinical and molecular diagnosis of WAS.

The MDS committee of the Japanese Society of Paediatric Hematology/Oncology (JSPHO) study coordinating center of the European Working Group of MDS in Childhood (EWOG-MDS) perform the morphological review of peripheral blood (PB) and BM smears and laboratory examinations for the diagnosis of JMML in Japan and Germany, respectively. By January 2011, WAS was diagnosed in six Japanese males (including patient #1) and one German male who were initially referred with a suspected diagnosis of JMML. Patient #4 was recently reported [21]. Approval for the study was obtained from the institutional review board of Nagoya University, Nagoya, Japan, and University of Freiburg, Freiburg, Germany. Informed consent was provided by parents according to the Declaration of Helsinki.

Diagnostic Tests for Wiskott–Aldrich Syndrome

Intracellular WASP expression in lymphocytes was analysed by flow cytometry (FCM) by the standard method described previously [4,22]. DNA purification and sequencing of genomic DNA, RNA isolation, reverse transcription-polymerase chain reaction, and sequencing of cDNA for the mutational analysis of *WASP* gene was performed as reported previously [23].

Diagnostic Tests for Juvenile Myelomonocytic Leukemia

Mutational screening for *PTPN11*, *NRAS*, and *KRAS* genes was performed in six patients, as previously reported [24–27]. In patients #6 and #7, the c-CBL gene, which has been recently found in about 10% of JMML patients, was also screened as described previously [16,18]. None of the patients had clinical signs of neurofibromatosis type 1 (NF1). *In vitro* colony assay for granulocyte–macrophage colony stimulating factor (GM-CSF) hypersensitivity assay was performed as a supportive diagnostic tool for JMML as previously reported [28,29].

RESULTS

Clinical Characteristics and Laboratory Findings

The clinical characteristics of these patients are summarized in Table I. Thrombocytopenia and bloody diarrhoea were observed soon after birth in all patients except for patient #6. JMML-like clinical manifestations occurred within the first few months of life. Eczema developed between 0 and 3 months after birth in all patients. Splenomegaly was seen in three of seven patients and massive splenomegaly was present in two patients. At the presentation of JMML-like features, episodes of recurrent infections, which suggest an immunodeficiency, were not observed in any patients. However, in three patients, recurrent bacterial, or viral infections (cases #5, #6, and #7) were documented during the clinical course.

The laboratory findings at the presentation of JMML-like disease are summarized in Table II. The WBC count was increased in all patients except for in patient #7. Monocytosis and myeloid/erythroid precursors were seen in PB in all patients. All patients had anaemia. The MPV before platelet transfusions ranged between 6.9 and 7.9 fl (normal, 7.2–11.7 fl) in the five patients that were evaluated. Hb F levels were normal in three patients examined. The platelet morphology demonstrated anisocytosis in all patients. Occasional giant platelets, which are defined as platelets bigger than red cells, were observed in six patients. These features were unusual for WAS. Full BM with significant predominance of myelopoiesis and a marked left shift of the myeloid lineage was seen in all patients. The number of megakaryocytes was normal or increased. Dysplasia in megakaryopoiesis, myelopoiesis, and erythropoiesis was observed in seven, four, and four patients, respectively. The common dysplasia in the megakaryopoiesis included hypolobulations of nuclei and small megakaryocytes with single or double round nuclei. In the myelopoiesis, nuclear abnormalities such as double nuclei, ring nuclei, or pseudo-Pelger–Huet anomaly nuclei were often seen. The dysplasia of erythropoiesis was mild, if observed, and included nuclear lobulation and double nuclei. The karyotype was normal in all patients. The serum levels of immunoglobulin were variable (Table II). Evaluation of T cell function revealed normal responses to phytohemagglutinin and concanavalin A in the four patients that were examined. The numbers of peripheral T and B cells and the CD4/8 ratio were normal in four patients. Patient #7 demonstrated B-lymphocytopenia and an elevated CD4/8 ratio.

Diagnostic Tests for Juvenile Myelomonocytic Leukemia

Molecular analysis of *PTPN11*, *N-RAS*, and *K-RAS* genes (n = 7) and the c-*CBL* gene (n = 2) documented no mutations in any of the examined patients. *In vitro* GM-CSF hypersensitivity was performed in all patients but patient #1 and was positive only in patient #4.

Diagnostic Tests for Wiskott–Aldrich Syndrome

FCM analysis showed absent (n = 6) or reduced (n = 1) WASP expression in the lymphocytes, which led to the confirmation of a diagnosis of WAS (Table III). Mutations of *WASP* genes

Pediatr Blood Cancer DOI 10.1002/pbc

TABLE I. Clinical Features of the Patients

Patient	1	2	3	4	5	6	7
Age at the detection of thrombocytopenia	At birth	At birth	At birth	At birth	1 month	4 months	2 months
Age at the onset of JMML like haematological features	1 month	3 months	1 month	1 month	1 month	4 months	2 months
Age at the onset of eczema	1 month	3 months	Soon after birth	3 months	1 month	3 months	2 months
Age at the onset of bloody diarrhoea	At birth	20 days	At birth	1 week	1 month	No	1 month
Hepatomegaly/splenomegaly (cm under the costal margin)	Yes (3)/no	Yes (3)/yes#	No/no	No/no	No/no	Yes (5)/yes (7.5)	Yes (6)/yes (6)
Infectious episodes before the diagnosis of WAS	CMV antigenemia	No episode	No episode	No episode	Fever of unknown origin	Otitis media	Adenovirus and Rotavirus in stool
Infectious episodes between the diagnosis of WAS and HSCT	No episode	No episode	No episode	No episode	Bacterial and RSV pneumonia Rotavirus gastroenteritis	Otitis media Anal abscess	CMV pneumonia
HSCT (age)	10 months	10 months	17 months	4 months	18 months	13 months	7 months
Donor/stem cell source	U-CBT	MSD-BMT	U-CBT	MSD-BMT	1 antigen MMUD-BMT	MUD-BMT	MUD-BMT
Survival (age at the time of the last follow-up)	Alive (6 years 5 months)	Alive (5 years 4 months)	Alive (4 years 8 months)	Alive (12 months)	Alive (1 year 9 months)	Alive (1 year 6 months)	Alive (1 year 7 months)

JMML, juvenile myelomonocytic leukaemia; WAS, Wiskott–Aldrich syndrome; RSV, respiratory syncytial virus; CMV, cytomegalovirus; # splenomegaly was noted only by ultrasound; HSCT, hematopoietic stem cell transplantation; U-CBT, unrelated cord blood transplantation; MSD-BMT, bone marrow transplantation from an HLA matched sibling donor; MUD-BMT, BMT from an HLA matched unrelated donor; MMUD-BMT, BMT from an HLA-mismatched unrelated donor.

TABLE II. Laboratory Findings Accompanying the Juvenile Myelomonocytic Leukaemia-Like Haematological Features

Patient	1	2	3	4	5	6	7
Peripheral blood							
WBC count ($\times 10^9$/L)	35.5–50.0	12.0–18.0	13.5–22.1	15.0	35.0–50.0	6.0–12.0	7.5
Monocyte count ($\times 10^9$/L)	8.9	1.0–1.5	8	2.3	1.1	1.0–1.5	1.3
Blasts (%)	3	2	2	4	2	0	1
Immature myeloid/erythroid cells	Yes/Yes	Yes/Yes	Yes/Yes	Yes/Yes	Yes/Yes	Yes/Yes	Yes/Yes
Eosinophils (%)	3	12	4	7	2	5	2
Platelet count ($\times 10^9$/L)	44	40–90	31	24	53	11	26
MPV (fl)[a]	7.0	7.4	NE	6.9	7.5	NE	7.9
Platelet anisocytosis/giant platelets	Yes/Yes	Yes/Yes	Yes/Yes	Yes/No	Yes/Yes	Yes/Yes	Yes/Yes
Hb (g/dl)	8.9	8.0	9.2	6.1	11.6	9.5	8.0
Bone marrow							
Cellularity	Full[b]	Full	Full	Full	Full	Full	Full
M/E ratio	33	4	7	5.4	11	2	2
Blasts (%)	3.5	0.5	1	0	2	3.5	2
Karyotype	46,XY	46,XY	46,XY	46, XY	46, XY	46,XY	46,XY
Immunological examination							
Age at examination (months)	8	5	2	2	10	4	2/3/5
IgG (mg/dl)	2,554	468	638	102	792	3,780	1,170/2,120/2,070
IgM (mg/dl)	156	64	37	<5	33	353	122/244/156
IgA (mg/dl)	49	52	38	39	129	124	25/45.4/58.2
IgE (mg/dl)	494	368	89	8	16	1,330 (10 months)	258/693/7,995
LBT (PHA, ConA)	Normal	Normal	NE	NE	NE	Normal	Normal
CD4/8 ratio	Normal	Normal	NE	Normal	NE	Normal	Increased (7.0/22.2/1.1)

WBC, white blood cell; MPV, mean platelet volume; M/E myeloid-/erythroid-cells; LBT, lymphoblastic test; PHA, phytohemagglutinin; conA, concanavalin A; NE, not evaluated. [a]Normal range (7.2–11.7 fl). [b]The cellularity was high (full bone marrow), which was normal for infants.

varied between patients. In patient #1, sequencing of *WASP* cDNA identified five nucleotides (CCGGG) inserted at position c.387 in exon 4, causing a frameshift at codon 140 that gave rise to a premature stop signal at codon 262, as reported previously [20]. Patients #2 and #3 had previously known nonsense mutations in exon 1 and exon 4, which led to the absence of WASP expression and a moderate to severe clinical phenotype of WAS [4,30–32]. Patient #4 had a known deletion in intron 8, which cause a frameshift and absence of WASP expression [4,5]. Patient #5 had a known splice anomaly in intron 6, which reduced expression of WASP and led to a clinical phenotype of either XLP or WAS [4,32]. Patient #6 had known deletion in exon 1, which was associated with a classic WAS phenotype [33]. Patient #7 had a nonsense mutation in exon 1, which has not been previously described.

Clinical Course of Patients

Patient #1 received 6-MP to control leukocytosis. In other patients, the JMML-like features were stable until allogeneic hematopoietic stem cell transplantation (HSCT), which was performed at the age of 4–18 months. All patients are alive after HSCT at the time of the last follow-up (Table I). Graft failure was observed in patient #7, and a second HSCT is currently planned for this patient.

DISCUSSION

Although WASP is expressed ubiquitously in hematopoietic cells and although *in vitro* results suggest that WASP is involved in the proliferation and differentiation of all hematopoietic progenitors, overt defects are restricted to micro-thrombocytopenia and immune-dysfunction in classical WAS. We previously described a case of a male presenting with a clinical picture of JMML, in whom WAS was ultimately diagnosed (patient #1) [20]. These haematological abnormalities had not been previously reported in patients with WAS. Since then, we have encountered six additional patients with WAS who presented with similar clinical characteristics. Morphological features were not distinguishable from JMML. Moreover, normal MPV and the presence

TABLE III. Results of the Diagnostic Tests for Wiskott–Aldrich Syndrome

Patient	1	2	3	4	5	6	7
Age at examinations	8 months	4 months	4 months	3 months	8 months	4 months	3 months
WASP protein expression	Absence	Absence	Absence	Absence	Reduced	Absence	Absence
WASP mutation	Exon 4 c.387–421 ins 5nt	Exon 1 c.37C>T	Exon 4 c.424C>T	Intron 8 c.777+1_+4 delGTGA	Intron 6 c.559+5G>A	Exon1 c.31delG	Exon 1 c.C55>T
Mutation type	Insertion	Nonsense	Nonsense	Deletion	Splice anomaly	Deletion	Nonsense
Predicted protein change	Frameshift stop aa 262	R13X	Q142X	Frameshift stop aa 246	Frameshift stop aa 190	Frameshift stop aa 37	Q19X

of giant platelets in three and six patients, respectively, initially argued against a diagnosis of WAS, because micro-thrombocytes are known as a key diagnostic feature of WAS and XLP. The JMML-like features developed shortly after birth in all patients, before the full clinical picture of WAS become apparent. In our patients with JMML-like features, signs of immune defects were not present. Without recent advances in molecular diagnostic tests for WAS and JMML, it might otherwise be impossible to establish a diagnosis of WAS in these patients. Absent or reduced WASP expression by FCM–WASP and detection of *WASP* mutation ultimately led to a diagnosis of WAS. The mutations were distributed in different exons and introns, and there was no clustering. Thrombocytopenia since birth and some of the observed clinical features (e.g., atopic dermatitis-like eczema, persistent bloody stool, lack of splenomegaly) were unusual for JMML but were compatible with WAS.

The deregulated RAS signalling pathway plays a central role in the pathogenesis of JMML, and mutational analyses of *PTPN11*, *RAS*, and *c-CBL* genes located in the RAS signalling pathway have become important diagnostic tests. Mutations of one of these genes and a clinical diagnosis of NF1 can be found in more than 80% of patients with JMML. However, in up to 20% of patients without any molecular markers, a diagnosis of JMML relies on unspecific clinical and laboratory observations. We suggest that WAS should be considered within the differential diagnosis in male infants with clinical features of JMML if no mutations of the RAS signalling pathway can be detected. Importantly, clinicians should not exclude a diagnosis of WAS if the MPV is normal or if giant platelets are present. Rarely, patients with WAS can present with normal or large platelets [34,35].

The pathogenesis of JMML-like feature in these patients is unknown. There is no evidence that WASP is related to the RAS signalling pathway. The activation of this pathway does not seem to be a major cause of JMML-like features in our patients, because GM-CSF hypersensitivity was demonstrated only in one of six patients examined. Patients with WAS have an increased risk of viral infections. CMV, Epstein–Barr virus (EBV) and human herpes virus-6 (HHV-6) infections can mimic JMML in infants [36,37]. However, extensive screening failed to detect viral infections at the time, at which these patients presented with JMML-like features, except for patient #1, in whom CMV antigen was detected.

Leukocyte adhesion deficiency (LAD)-1 is a rare immunodeficiency caused by a mutation in the beta-2 integrin gene. The firm adhesion of leukocyte to the blood vessel wall is defective in LAD-1, which results in leukocytosis, mimicking JMML [38]. A defect of leukocyte adhesion due to abnormal integrin beta clustering has been described in the context of WAS [39]. A mechanism similar to that seen in LAD1 may be present in WAS with JMML-like features.

A recent report showed that WASP localizes to not only the cytoplasm but also to the nucleus and has a role in the transcriptional regulation at the chromatin level in lymphocytes [40]. Active *WASP* mutations, which cluster within the GTP-ase binding domain of WASP (L270P, S272P, and I294T), cause XLN and myelodysplasia [6,7]. Further, increased apoptosis associated with increased genomic instability in myeloid cells and lymphocytes has been described in the context of active *WASP* mutations [41,42]. Further research may identify new roles of WASP in transcriptional regulation and genomic stability in haematopoiesis, which may explain the JMML-like features, seen in WAS patients.

In conclusion, WAS should be considered in the differential diagnosis in male infants presenting with JMML-like features if no molecular markers of JMML can be demonstrated. A normal MPV and the presence of giant platelets do not exclude a diagnosis of WAS. Clinical information, such as bloody stool and eczema, may be helpful in pursuing a diagnosis of WAS in an infant with JMML like features.

ACKNOWLEDGMENT

We thank the members of the MDS committee of the JSPHO and the EWOG-MDS. We also thank Dr. Masahumi Onodera (National Medical Center for Children and Mothers Research Institute, Tokyo, Japan) and Dr. Klaus Schwarz (Institute for Transfusion Medicine, University of Ulm, Ulm, Germany) for the mutational analysis of the *WASP* gene in patients #5 and #7, respectively. We also thank Dr. Eva Jacobsen and Dr. Ansgar Schulz (Department of Paediatrics and Adolescent Medicine, University Hospital Ulm, Ulm, Germany) for FACS analysis of WASP expression in patient #7 and thank Dr. Kenichi Koike (Shinshu University School of Medicine, Matsumoto, Japan), Dr. Christian Flotho and Dr. Thomas Gorr for the mutational analysis of *PTPN11*, *RAS*, *c-CBL* gens in patients #6 and #7.

REFERENCES

1. Bosticardo M, Marangoni F, Aiuti A, et al. Recent advances in understanding the pathophysiology of Wiskott–Aldrich syndrome. Blood 2009;113:6288–6295.
2. Thrasher AJ, Burns SO. WASP: A key immunological multitasker. Nat Rev Immunol 2010;10: 182–192.
3. Derry JM, Ochs HD, Francke U. Isolation of a novel gene mutated in Wiskott–Aldrich syndrome. Cell 1994;78:635–644.
4. Imai K, Morio T, Zhu Y, et al. Clinical course of patients with WASP gene mutations. Blood 2004;103:456–464.
5. Jin Y, Mazza C, Christie JR, et al. Mutations of the Wiskott–Aldrich syndrome protein (WASP): Hotspots, effect on transcription, and translation and phenotype/genotype correlation. Blood 2004;104:4010–4019.
6. Devriendt K, Kim AS, Mathijs G, et al. Constitutively activating mutation in WASP causes X-linked severe congenital neutropenia. Nat Genet 2001;27:313–317.
7. Ancliff PJ, Blundell MP, Cory GO, et al. Two novel activating mutations in the Wiskott–Aldrich syndrome protein result in congenital neutropenia. Blood 2006;108:2182–2189.
8. Hasle H, Wadsworth LD, Massing BG, et al. A population-based study of childhood myelodysplastic syndrome in British Columbia, Canada. Br J Haematol 1999;106:1027–1032.
9. Baumann I, Benett J, Niemeyer CM, et al. Juvenile myelomonocytic leukemia. In: Swerdlow S, Campo E, Harris N, et al, editors. WHO classification of tumors of haematopoietic and lymphoid tissues. Lyon: IARC Press; 2008. 82–86.
10. Niemeyer CM, Arico M, Basso G, et al. Chronic myelomonocytic leukemia in childhood: A retrospective analysis of 110 cases. European Working Group on Myelodysplastic Syndromes in Childhood (EWOG-MDS). Blood 1997;89:3534–3543.
11. Yoshimi A, Kojima S, Hirano N. Juvenile myelomonocytic leukemia: Epidemiology, etiopathogenesis, diagnosis, and management considerations. Paediatr Drugs 2010;12:11–21.
12. Tartaglia M, Niemeyer CM, Song X, et al. Somatic *PTPN11* mutations in juvenile myelomonocytic leukemia, myelodysplastic syndromes and acute myeloid leukemia. Nat Genet 2003;34:148–150.
13. Flotho C, Valcamonica S, Mach-Pascula S, et al. RAS mutations and clonality analysis in children with juvenile myelomonocytic leukemia (JMML). Leukemia 1999;13:32–37.
14. Side L, Taylor B, Cayouette M, et al. Homozygous inactivation of the NF1 gene in bone marrow cells from children with neurofibromatosis type 1 and malignant myeloid disorders. N Engl J Med 1997;336:1713–1720.
15. Le DT, Kong N, Zhu Y, et al. Somatic inactivation of *Nf1* in hematopoietic cells results in a progressive myeloproliferative disorder. Blood 2004;103:4243–4250.
16. Niemeyer CM, Kang MW, Shin DH, et al. Germline CBL mutations cause developmental abnormalities and predispose to juvenile myelomonocytic leukemia. Nat Genet 2010;42:794–800.
17. Loh ML, Sakai DS, Flotho C, et al. Mutations in CBL occur frequently in juvenile myelomonocytic leukemia. Blood 2009;114:1859–1863.
18. Muramatsu H, Makishima H, Jankowska AM, et al. Mutations of an E3 ubiquitin ligase c-Cbl but not TET2 mutations are pathogenic in juvenile myelomonocytic leukemia. Blood 2010;115: 1969–1975.
19. Kajiwara M, Nonoyama S, Eguchi M, et al. WASP is involved in proliferation and differentiation of human haemopoietic progenitors in vitro. Br J Haematol 1999;107:254–262.
20. Watanabe N, Yoshimi A, Kamachi Y, et al. Wiskott–Aldrich syndrome is an important differential diagnosis in male infants with juvenile myelomonocytic leukemialike features. J Pediatr Hematol Oncol 2007;29:836–838.
21. Sano H, Kobayashi R, Suzuki D, et al. Wiskott–Aldrich syndrome with unusual clinical features similar to juvenile myelomonocytic leukemia. Int J Hematol 2012;96:279–283.
22. Yamada M, Ariga T, Kawamura N, et al. Determination of carrier status for the Wiskott–Aldrich syndrome by flow cytometric analysis of Wiskott–Aldrich syndrome protein expression in peripheral blood mononuclear cells. J Immunol 2000;165:1119–1122.
23. Itoh S, Nonoyama S, Morio T, et al. Mutations of the WASP gene in 10 Japanese patients with Wiskott–Aldrich syndrome and X-linked thrombocytopenia. Int J Hematol 2000;71:79–83.

24. Yoshida N, Yagasaki H, Xu Y, et al. Correlation of clinical features with the mutational status of GM-CSF signaling pathway-related genes in juvenile myelomonocytic leukemia. Pediatr Res 2009;65: 334–340.
25. Yamamoto T, Isomura M, Xu Y, et al. PTPN11, RAS and FLT3 mutations in childhood acute lymphoblastic leukemia. Leuk Res 2006;30:1085–1089.
26. Mitani K, Hangaishi A, Imamura N, et al. No concomitant occurrence of the N-ras and p53 gene mutations in myelodysplastic syndromes. Leukemia 1997;11:863–865.
27. Tartaglia M, Martinelli S, Cazzaniga G, et al. Genetic evidence for lineage-related and differentiation stage-related contribution of somatic PTPN11 mutations to leukemogenesis in childhood acute leukemia. Blood 2004;104:307–313.
28. Emanuel PD, Bates LJ, Castleberry RP, et al. Selective hypersensitivity to granulocyte–macrophage colony-stimulating factor by juvenile chronic myeloid leukemia hematopoietic progenitors. Blood 1991;77:925–929.
29. Emanuel PD, Bates LJ, Zhu SW, et al. The role of monocyte-derived hemopoietic growth factors in the regulation of myeloproliferation in juvenile chronic myelogenous leukemia. Exp Hematol 1991;19: 1017–1024.
30. Jo EK, Futatani T, Kanegane H, et al. Mutational analysis of the WASP gene in 2 Korean families with Wiskott–Aldrich syndrome. Int J Hematol 2003;78:40–44.
31. Qasim W, Gilmour KC, Heath S, et al. Protein assays for diagnosis of Wiskott–Aldrich syndrome and X-linked thrombocytopenia. Br J Haematol 2001;113:861–865.
32. Lemahieu V, Gastier JM, Francke U. Novel mutations in the Wiskott–Aldrich syndrome protein gene and their effects on transcriptional, translational, and clinical phenotypes. Hum Mutat 1999;14:54–66.
33. Ariga T, Yamada M, Sakiyama Y. Mutation analysis of five Japanese families with Wiskott–Aldrich syndrome and determination of the family members' carrier status using three different methods. Pediatr Res 1997;41:535–540.
34. Patel PD, Samanich JM, Mitchell WB, et al. A unique presentation of Wiskott–Aldrich syndrome in relation to platelet size. Pediatr Blood Cancer 2011;56:1127–1129.
35. Knox-Macaulay HH, Bashawri L, Davies KE. X linked recessive thrombocytopenia. J Med Genet 1993;30:968–969.
36. Manabe A, Yoshimasu T, Ebihara Y, et al. Viral infections in juvenile myelomonocytic leukemia: Prevalence and clinical implications. J Pediatr Hematol Oncol 2004;26:636–641.
37. Herrod HG, Dow LW, Sullivan JL. Persistent Epstein–Barr virus infection mimicking juvenile chronic myelogenous leukemia: Immunologic and hematologic studies. Blood 1983;61:1098–1104.
38. Karow A, Baumann I, Niemeyer CM. Morphologic differential diagnosis of juvenile myelomonocytic leukemia–pitfalls apart from viral infection. J Pediatr Hematol Oncol 2009;31:380.
39. Zhang H, Schaff UY, Green CE, et al. Impaired integrin-dependent function in Wiskott–Aldrich syndrome protein-deficient murine and human neutrophils. Immunity 2006;25:285–295.
40. Taylor MD, Sadhukhan S, Kottangada P, et al. Nuclear role of WASp in the pathogenesis of dysregulated TH1 immunity in human Wiskott–Aldrich syndrome. Sci Transl Med 2010;2:37ra44.
41. Westerberg LS, Meelu P, Baptista M, et al. Activating WASP mutations associated with X-linked neutropenia result in enhanced actin polymerization, altered cytoskeletal responses, and genomic instability in lymphocytes. J Exp Med 2010;207:1145–1152.
42. Moulding DA, Blundell MP, Spiller DG, et al. Unregulated actin polymerization by WASp causes defects of mitosis and cytokinesis in X-linked neutropenia. J Exp Med 2007;204:2213–2224.

Genetic correction of *HAX1* in induced pluripotent stem cells from a patient with severe congenital neutropenia improves defective granulopoiesis

Tatsuya Morishima,[1] Ken-ichiro Watanabe,[1] Akira Niwa,[2] Hideyo Hirai,[3] Satoshi Saida,[1] Takayuki Tanaka,[2] Itaru Kato,[1] Katsutsugu Umeda,[1] Hidefumi Hiramatsu,[1] Megumu K. Saito,[2] Kousaku Matsubara,[4] Souichi Adachi,[5] Masao Kobayashi,[6] Tatsutoshi Nakahata,[2] and Toshio Heike[1]

[1]Department of Pediatrics, Graduate School of Medicine, Kyoto University, Kyoto; [2]Department of Clinical Application, Center for iPS Cell Research and Application, Kyoto University, Kyoto; [3]Department of Transfusion Medicine and Cell Therapy, Kyoto University Hospital, Kyoto; [4]Department of Pediatrics, Nishi-Kobe Medical Center, Kobe; [5]Human Health Sciences, Graduate School of Medicine, Kyoto University, Kyoto; and [6]Department of Pediatrics, Hiroshima University Graduate School of Biomedical Sciences, Hiroshima, Japan

ABSTRACT

HAX1 was identified as the gene responsible for the autosomal recessive type of severe congenital neutropenia. However, the connection between mutations in the *HAX1* gene and defective granulopoiesis in this disease has remained unclear, mainly due to the lack of a useful experimental model for this disease. In this study, we generated induced pluripotent stem cell lines from a patient presenting for severe congenital neutropenia with *HAX1* gene deficiency, and analyzed their *in vitro* neutrophil differentiation potential by using a novel serum- and feeder-free directed differentiation culture system. Cytostaining and flow cytometric analyses of myeloid cells differentiated from patient-derived induced pluripotent stem cells showed arrest at the myeloid progenitor stage and apoptotic predisposition, both of which replicated abnormal granulopoiesis. Moreover, lentiviral transduction of the *HAX1* cDNA into patient-derived induced pluripotent stem cells reversed disease-related abnormal granulopoiesis. This *in vitro* neutrophil differentiation system, which uses patient-derived induced pluripotent stem cells for disease investigation, may serve as a novel experimental model and a platform for high-throughput screening of drugs for various congenital neutrophil disorders in the future.

Introduction

Severe congenital neutropenia (SCN) is a rare myelopoietic disorder resulting in recurrent life-threatening infections due to a lack of mature neutrophils,[1] and individuals with SCN present for myeloid hypoplasia with an arrest of myelopoiesis at the promyelocyte/myelocyte stage.[1,2] SCN is actually a multigene syndrome that can be caused by inherited mutations in several genes. For instance, approximately 60% of SCN patients are known to carry autosomal dominant mutations in the *ELANE* gene, which encodes neutrophil elastase (NE).[3] An autosomal recessive type of SCN was first described by Kostmann in 1956,[4] and defined as Kostmann disease. Although the gene responsible for this classical type of SCN remained unknown for more than 50 years, Klein *et al.* identified mutations in *HAX1* to be responsible for this type of SCN in 2007.[5] HAX1 localizes predominantly to mitochondria, where it controls inner mitochondrial membrane potential ($\Delta\psi_m$) and apoptosis.[6,7] Although an increase in apoptosis in mature neutrophils was presumed to cause neutropenia in HAX1 gene deficiency,[5] the connection between *HAX1* gene mutations and defective granulopoiesis in SCN has remained unclear.

To control infections, SCN patients are generally treated with granulocyte colony-stimulating factor (G-CSF); however, long-term G-CSF therapy associates with an increased risk of myelodysplastic syndrome and acute myeloid leukemia (MDS/AML).[8,9] Although hematopoietic stem cell transplantations are available as the only curative therapy for this disease, they can result in various complications and mortality.[4]

Many murine models of human congenital and acquired diseases are invaluable for disease investigation as well as for novel drug discoveries. However, their use in a research setting can be limited if they fail to mimic strictly the phenotype of the human disease in question. For instance, the *Hax1* knock-out mouse is characterized by lymphocyte loss and neuronal apoptosis, but not neutropenia.[10] Thus, it is not a suitable experimental model for SCN. Induced pluripotent stem (iPS) cells are reprogrammed somatic cells with embryonic stem (ES) cell-like characteristics produced by the introduction of specific transcription factors,[11,16] and they may substitute murine models of human disease. It is believed that iPS cell technology, which generates disease-specific pluripotent stem cells in combination with directed cell differentiation, will contribute enormously to patient-oriented research, including disease pathophysiology, drug screening, cell transplantation, and gene therapy.

In vitro neutrophil differentiation systems, which can reproduce the differentiation of myeloid progenitor cells to mature neutrophils, are needed to understand the pathogenesis of SCN better. Recently, we established a neutrophil differentia-

 doi:10.3324/haematol.2013.083873
The online version of this article has a Supplementary Appendix.
Manuscript received on January 9, 2013. Manuscript accepted on August 20, 2013.
Correspondence: heike@kuhp.kyoto-u.ac.jp

tion system from human iPS cells[17] as well as a serum- and feeder-free monolayer hematopoietic culture system from human ES and iPS cells.[18] In this study, we generate iPS cell lines from an SCN patient with *HAX1* gene deficiency and differentiate them into neutrophils *in vitro*. Furthermore, we corrected for the *HAX1* gene deficiency in HAX1-iPS cells by lentiviral transduction with *HAX1* cDNA and analyzed the neutrophil differentiation potential of these cells. Thus, this *in vitro* neutrophil differentiation system from patient-derived iPS cells may be a useful model for future studies in SCN patients with *HAX1* gene deficiency.

Methods

Human iPS cell generation

Skin biopsy specimens were obtained from an 11-year old male SCN patient with *HAX1* gene deficiency.[19] This study was approved by the Ethics Committee of Kyoto University, and informed consent was obtained from the patient's guardians in accordance with the Declaration of Helsinki. Fibroblasts were expanded in DMEM (Nacalai Tesque, Inc., Kyoto, Japan) containing 10% FBS (vol/vol, Invitrogen, Carlsbad, CA, USA) and 0.5% penicillin and streptomycin (wt/vol, Invitrogen). Generation of iPS cells was performed as described previously.[12] In brief, we introduced *OCT3/4, SOX2, KLF4,* and *cMYC* using ecotropic retroviral transduction into patient's fibroblasts expressing mouse *Slc7a1*. Six days after transduction, cells were harvested and re-plated onto mitotically inactive SNL feeder cells. On the following day, DMEM was replaced with primate ES cell medium (ReproCELL, Kanagawa, Japan) supplemented with basic fibroblast growth factor (5 ng/mL, R&D Systems, Minneapolis, MN, USA). Three weeks later, individual colonies were isolated and expanded.

Maintenance of cells

Control ES (KhES-1) and control iPS (253G4 and 201B6) cells were kindly provided by Drs. Norio Nakatsuji and Shinya Yamanaka (Kyoto University, Kyoto, Japan), respectively. These human ES and iPS cell lines were maintained on mitomycin-C (Kyowa Hakko Kirin, Tokyo, Japan)-treated SNL feeder cells as described previously[17] and subcultured onto new SNL feeder cells every seven days.

Flow cytometric analysis

Cells were stained with antibodies as reported previously.[17] Samples were analyzed using an LSR flow cytometer and Cell Quest software (Becton-Dickinson).

Neutrophil differentiation of iPS cells

In a previous study, we established a serum and feeder-free monolayer hematopoietic culture system from human ES and iPS cells.[18] In this study, we modified this culture system to direct neutrophil differentiation. iPS cell colonies were cultured on growth factor-reduced Matrigel (Becton-Dickinson)-coated cell culture dishes in Stemline II hematopoietic stem cell expansion medium (Sigma-Aldrich, St. Louis, MO, USA) containing the insulin-transferrin-selenium (ITS) supplement (Invitrogen) and cytokines. iPS cells were treated with cytokines as follows: bone morphogenetic protein (BMP) 4 (20 ng/mL, R&D Systems) was added for four days and then replaced with vascular endothelial growth factor (VEGF) 165 (40 ng/mL, R&D Systems) on Day 4. On Day 6, VEGF 165 was replaced with a combination of stem cell factor (SCF, 50 ng/mL, R&D Systems), interleukin (IL)-3 (50 ng/mL, R&D Systems), thrombopoietin (TPO, 5 ng/mL, kindly provided by Kyowa Hakko Kirin), and G-CSF (50 ng/mL, also kindly provided by Kyowa Hakko Kirin). Thereafter, medium was replaced every five days.

Dead cell removal and CD45$^+$ leukocyte separation

Floating cells were collected, followed by the removal of dead cells and cellular debris with the Dead Cell Removal kit (Miltenyi Biotec, Bergisch Gladbach, Germany). CD45$^+$ cells were then separated using human CD45 microbeads (Miltenyi Biotec). Cell separation procedures were performed using the autoMACS Pro Separator (Miltenyi Biotec).

Statistical analysis

Statistical analysis was carried out using Student's t-test. $P<0.05$ was considered statistically significant.

Results

Generation of iPS cell lines from an SCN patient with HAX1 gene deficiency

To generate patient-derived iPS cell lines, dermal fibroblasts were obtained from a male SCN patient with a homozygous 256C-to-T transition resulting in an R86X mutation in the *HAX1* gene.[19] These fibroblasts were reprogrammed to iPS cells after transduction with retroviral vectors encoding *OCT3/4, SOX2, KLF4* and *cMYC*,[12] and a total of 11 iPS cell clones were obtained. From these, we randomly selected three clones for propagation and subsequent analyses. One of these clones (HAX1 4F5) was generated with four factors (*OCT3/4, SOX2, KLF4*, and *cMYC*); the remaining clones (HAX1 3F3 and 3F5) were generated with three factors (*OCT3/4, SOX2*, and *KLF4*).[12]

All of these patient-derived iPS cell clones showed a characteristic human ES cell-like morphology (Figure 1A), and they propagated for serial passages in human ES cell maintenance culture medium. Quantitative PCR analysis showed the expression of *NANOG*, a pluripotent marker gene, to be comparable to that of control ES (KhES-1) and iPS (253G4 and 201B6) cells (Figure 1B). Surface marker analysis indicated that they were also positive for SSEA4, a human ES and iPS cell marker (Figure 1C). DNA sequencing analysis verified an identical mutation in the *HAX1* gene in all established iPS cell clones (Figure 1D). The pluripotency of all iPS cell clones was confirmed by the presence of cell derivatives representing all three germ layers by teratoma formation after subcutaneous injection of undifferentiated iPS cells into immunocompromised NOD/SCID/γc^{null} mice (Figure 1E).

To validate the authenticity of iPS cells further, we investigated the expression of the four genes that were used for iPS cell generation. The expression level of all endogenous genes was comparable to control ES and iPS cells. On the other hand, transgene expression was largely undetectable in patient-derived iPS cell clones (*Online Supplementary Figure S1A*). Chromosomal analysis revealed that all patient-derived iPS cell clones maintained a normal karyotype (*Online Supplementary Figure S1B*). Genetic identity was shown by short tandem repeat analysis (*Online Supplementary Figure S1C*).

Taken collectively, these results indicate that iPS cell clones were comprised of good quality iPS cells derived from the somatic cells of an SCN patient with *HAX1* gene deficiency (HAX1-iPS cells).

Maturation arrest at the progenitor level in neutrophil differentiation from HAX1-iPS cells

The paucity of mature neutrophils in the peripheral blood and a maturation arrest at the promyelocyte/myelocyte stage in the bone marrow are characteristic laboratory findings presented in the SCN patients with *HAX1* gene deficiency. To investigate whether our patient-derived iPS cell model accurately replicated this disease phenotype, we assessed neutrophil differentiation from HAX1-iPS cells by using a serum- and feeder-free monolayer culture system[18] with minor modifications (Online *Supplementary Figure S2*).

In this system, we cultured iPS cell colonies on Matrigel-coated dishes in serum-free medium supplemented with several cytokines and obtained hematopoietic cells as floating cells on approximately Day 26 of differentiation. May-Giemsa staining of floating live CD45$^+$ cells derived from normal iPS cells showed that approximately 40% were mature neutrophils (Figure 2A and B). The remaining cells consisted of immature myeloid cells as well as a small number of macrophages. Cells of other lineages such as erythroid or lymphoid cells were not observed. On the other hand, HAX1-iPS cell-derived blood cells contained only approximately 10% mature neutrophils and approxi-

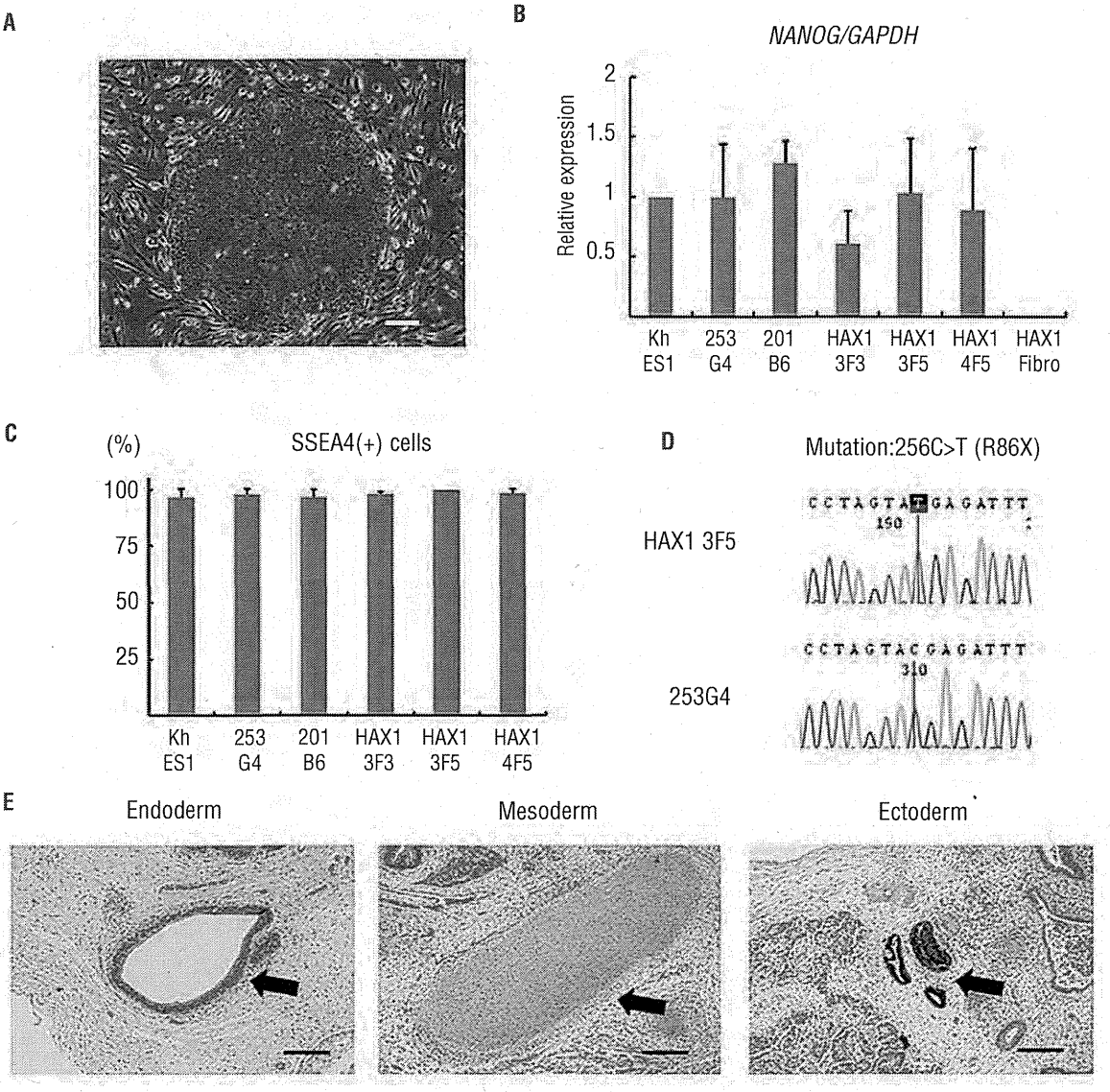

Figure 1. Generation of iPS cell lines from an SCN patient with *HAX1* gene deficiency. (A) Human ES cell-like morphology of HAX1-iPS cells. Scale bar: 200 μm. (B) *NANOG* expression in HAX1-iPS cells, control iPS cells (253G4 and 201B6), and patient-derived fibroblasts (HAX1 Fibro) compared to control ES cells (KhES1). *GAPDH* was used as an internal control (n = 3; bars represent SDs). (C) SSEA-4 expression analysis using flow cytometry. Gated on TRA1-85$^+$DAPI$^-$ cells as viable human iPS (ES) cells (n = 3; bars represent SDs). (D) DNA sequencing analysis of the *HAX1* gene in iPS cells. HAX1-iPS cells showed 256C>T (R86X) mutation that was found in the patient. (E) Teratoma formation from HAX1-iPS cells in the NOD/SCID/γc^{null} (NOG) mouse. Arrows indicate the following; Endoderm: respiratory epithelium; Mesoderm: cartilage; Ectoderm: pigmented epithelium. Scale bars: 200 μm. (A, D-E) Representative data (HAX1 3F5) are shown.

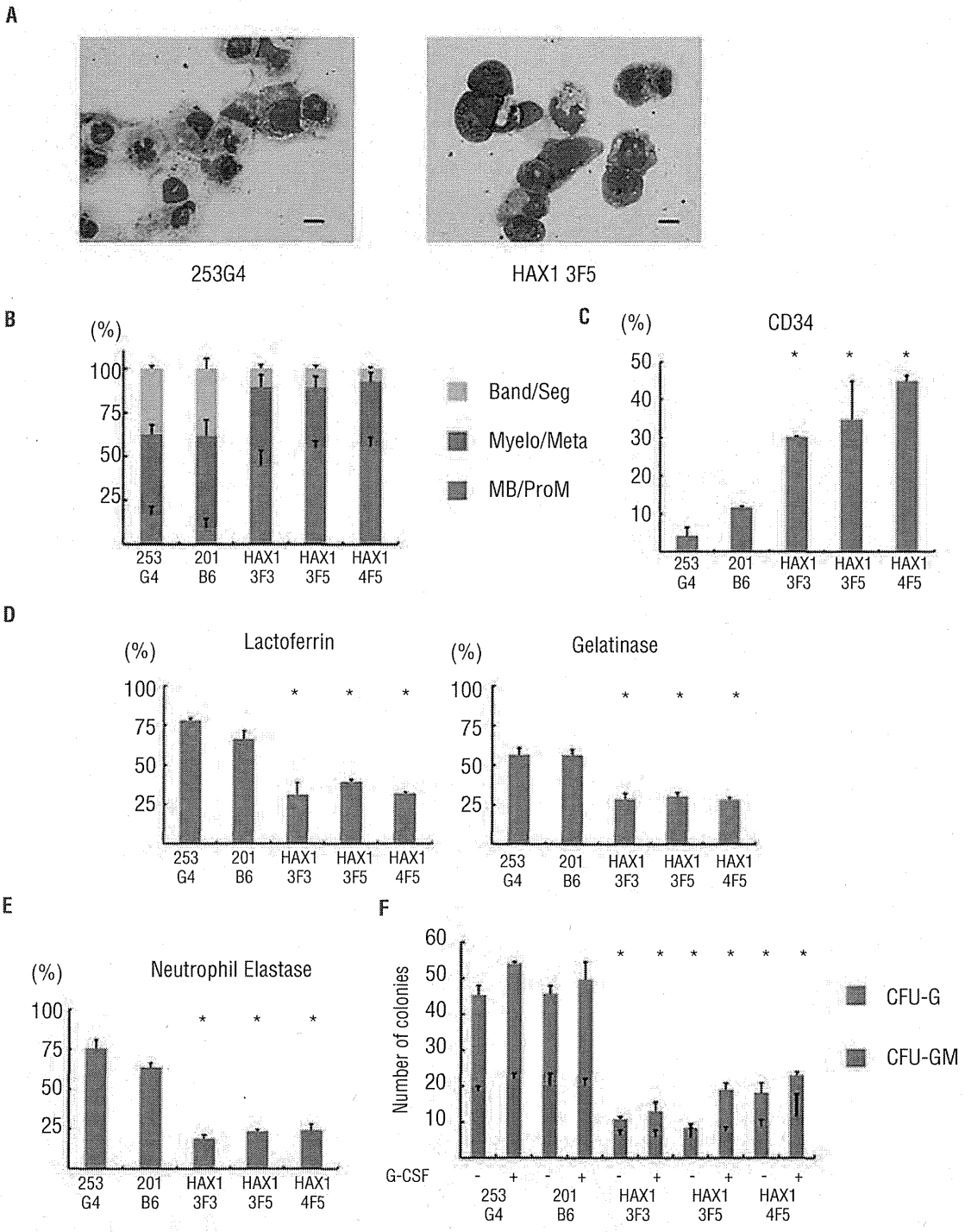

Figure 2. Maturation arrest at the progenitor level in neutrophil differentiation from HAX1-iPS cells. (A) May-Giemsa staining of CD45$^+$ cells derived from normal (253G4) and HAX1-iPS (HAX1 3F5) cells. Scale bars: 10 μm. (B) Morphological classification of CD45$^+$ cells derived from iPS cells. Cells were classified into three groups: myeloblast and promyelocyte (MB/ProM), myelocyte and metamyelocyte (Myelo/Meta), and band and segmented neutrophils (Band/Seg) (n = 3; bars represent SDs). (C) Flow cytometric analysis of CD45$^+$ cells derived from iPS cells. Cells gated on human CD45$^+$ DAPI$^-$ were analyzed (n = 3; bars represent SDs; *P<0.05 compared to control iPS cells). (D) Immunocytochemical analysis of CD45$^+$ cells derived from iPS cells (n = 3; bars represent SDs; *P<0.05 compared to control iPS cells). (E) NE staining of CD45$^+$ cells derived from iPS cells (n = 3; bars represent SDs; *P<0.05 compared to control iPS cells). (F) Colony-forming assay of cells derived from iPS cells. On Day 16, living adherent cells were collected and cultured in methylcellulose medium (see *Online Supplementary Appendix*). The number of colonies generated from 1×10^4 cells is indicated (n = 3; bars represent SD; *P<0.05 compared to control iPS cells). (A–E) Live CD45$^+$ cells derived from normal and HAX1-iPS cells on Day 26 of neutrophil differentiation were analyzed. Dead cells and CD45$^-$ cells were depleted using an autoMACS Pro separator (see *Methods*).